Tribology Transactions

ISSN: 1040-2004 (Print) 1547-397X (Online) Journal homepage: http://www.tandfonline.com/loi/utrb20

A Review of Elasto-Hydrodynamic Lubrication Theory

P. M. Lugt & G. E. Morales-Espejel

To cite this article: P. M. Lugt & G. E. Morales-Espejel (2011) A Review of Elasto-Hydrodynamic Lubrication Theory, Tribology Transactions, 54:3, 470-496, DOI: 10.1080/10402004.2010.551804

To link to this article: https://doi.org/10.1080/10402004.2010.551804

Tribology Transactions, 54: 470-496, 2011

ISSN: 1040-2004 print / 1547-397X online
DOI: 10.1080/10402004.2010.551804

STLE
Society of Tribologists and Lubrication Engineers

A Review of Elasto-Hydrodynamic Lubrication Theory

P. M. LUGT[1] and G. E. MORALES-ESPEJEL[1,2]
[1]SKF Engineering & Research Centre
P.O. Box 2350, 3430 DT Nieuwegein
The Netherlands
[2]Université de Lyon, INSA-Lyon, CNRS
LaMCoS UMR5259
F69621, Lyon France

The development and understanding of elastohydrodynamic lubrication (EHL) can be traced back to the beginning of the previous century. However, it was not until 1949 that the first real solution of the problem was published. Since then, the technology has evolved enormously. In the current article a summary of these developments is given. Smooth surface EHL has become well established. Numerical methods, analytical solutions, and experimental techniques have become mature. Focus areas of research today are thermal EHL, starved EHL, friction (non-Newtonian lubricants), roughness, and grease. The scope of EHL is so wide that the authors needed select the topics of focus in this article. Therefore, in addition to the general overview of the areas of friction, analytical methods, starved EHL, and grease EHL are highlighted in this article.

KEY WORDS

Elasto-Hydrodynamic Lubrication; Starvation; Friction

INTRODUCTION

In recent times, industry has faced increasing pressure to improve the design of mechanical components in order to deal with new requirements from the market and legislation. Engineers are often confronted with increasing demands of less expensive, more efficient, and environmentally friendly products. Mechanical contacts (dry and lubricated) have particularly suffered from this. It is well known that many mechanical components have seen an increasing shift of failures from the component body to their interfaces (contacting surfaces). This is particularly true with rolling/sliding surfaces, mainly lubricated. Thinner lubricating films are often used (e.g., Dowson *(1)*); thus, surface topography becomes very relevant in the life of the component. Often, environmental pressure pushes engineers to produce complete new designs, reduce friction, and extend the life in elastohydrodynamic lubrication (EHL) contacts, which requires a sound understanding of the physical phenomena and capabilities for prediction, which is usually done through modeling.

These increasing demands have led to a continuous interest in the area of elastohydrodynamic lubrication throughout the years and the number of publications in this area is large. The present article gives a review of this technology. Due to the very large number of publications, this review is far from complete. The authors have therefore chosen to briefly summarize the various aspects only and to go into somewhat more detail in the area around their own work. The article is concluded by a summary and outlook/recommendations for future research.

DEFINITION OF EHL

Elastohydrodynamic lubrication is the type of lubrication that occurs in lubricated contraformal contacts where the elastic deformation of the lubricated surfaces has a substantial influence on the thickness of the lubricating film. Such contacts occur in, for example, rolling bearings, cam-tappet systems, gears, flexible seals, and human synovial joints. The elastic deformation is caused by the high pressures in such contacts, which in general also cause a substantial increase of viscosity. Both effects have a positive influence on the thickness of the lubricant film.

HISTORY

The history of elastohydrodynamic lubrication goes back to 1886, when Reynolds published his famous article where he derived the differential equation describing the pressure distribution and load-carrying capacity of lubricating films for journal bearings *(2)*. In 1916, Martin *(6)* and Gümbel *(7)* applied Reynolds' equation to the lubrication of gears and found film thicknesses that were too small to explain the full-film lubrication that was observed here. In 1941 Meldahl *(9)* included elastic deformations caused by the contact pressures, but still the film thickness predictions were too small. In 1945 Ertel *(10)* (published under the name of Grubin *(12)* in 1949, see Cameron *(14)*), included a pressure–viscosity effect on the film thickness and finally a full film could be predicted. Since then this type of lubrication has been called *elasto hydrodynamic lubrication* (EHL). Formulae for line contacts, based on numerical calculations, were developed by Petrusevich *(15)* and Dowson and Higginson *(18)*, *(19)*. In 1972 Kauzlarich and Greenwood *(20)* solved the line

Manuscript received December 13, 2010
Manuscript accepted December 30, 2010
Review led by Farshid Sadeghi

NOMENCLATURE

a = Half-width of the elliptical Hertzian contact, rolling direction (m)
B = Bulk modulus of the lubricant (Pa)
b = Half-width of the elliptical Hertzian contact, transverse direction (m)
C = Constant in the Crook film thickness shape
d = Distance between the center of the flat area and the center of the contact (m)
d_e = Elastic deformation (m)
E' = Reduced elasticity modulus, $E' = 2\left(\frac{1-\nu_1^2}{E_1} + \frac{1-\nu_2^2}{E_2}\right)^{-1}$ (Pa)
F = Normal load (N)
h = Film thickness (m)
$\tilde{h}$ = Combined oil layer thickness (m)
h^* = Film thickness (Ertel-Grubin analysis) at $dp/dx = 0$ (m)
h_c = Central film thickness (m)
h_{cs} = Central film thickness, starved (m)
h_{cff} = Central film thickness, fully flooded lubrication (m)
$h_{isothermal}$ = Film thickness excluding inlet shear heating effect (m)
h_o = Constant in film thickness equation (m)
$h_{thermal}$ = Film thickness including inlet shear heating effect (m)
$\hat{H}^*$ = Dimensionless film thickness (Ertel-Grubin analysis) at $dp/dx = 0$ (m)
$\hat{H}$ = Dimensionless film thickness (Ertel-Grubin analysis) $\hat{H} = 2R_x h/a^2$
$\hat{H}_c$ = Dimensionless central film thickness (Ertel-Grubin analysis, $\hat{H}_c = \hat{H}^*$)
H_0 = Dimensionless central film thickness (Greenwood, $H_0 = 4R_x h^*/a^2$)
K = Dimensionless number (Ertel-Grubin analysis) $K = 48\bar{u}\eta_o R_x^2/(a^3 p_o)$
K_1 = Dimensionless number (Ertel-Grubin analysis) $K_1 = \alpha p_o$
K = Grease "consistency" [Pa s^n]
K_0 = Grease "consistency" at ambient pressure (Pa s^n)
K_2 = Grease "consistency" at ambient pressure (Pa s^n)
k = Thermal conductivity (lubricant or solid wall) (W $m^{-1}K^{-1}$))
k_{grease} = Thermal conductivity grease (W $m^{-1}K^{-1}$))
k_{oil} = Thermal conductivity oil (W $m^{-1}K^{-1}$))
L = Dimensionless inlet length $L = l/a$
L = Moes dimensionless lubricant number $L = \alpha E' \left(\frac{E' R_x}{\eta_0 u_s}\right)^{-\frac{1}{4}}$
l = Inlet length (m)
l_t = Total length of the tracks (m)
M = Moes dimensional load number $M = \frac{F}{E' R_x^2}\left(\frac{E' R_x}{\eta_0 u_s}\right)^{\frac{3}{4}}$
m = Mass (kg)
n = Number of overrollings
n = Power law exponent
n_x, n_y = Number of nodes in x and y direction
P = Dimensionless pressure $P = p/p_o$
p = Pressure (Pa)
p_r = Reference pressure (Pa)
p_o = Maximum Hertzian pressure (Pa)
p_m = Mean Hertzian pressure (Pa)
p_L = Inlet pressure (Pa)
p_R = Outlet pressure (Pa)
Q = Reduced dimensionless pressure $Q = q/p_o$
Q_s = Reduced dimensionless pressure $Q = q/p_o$ at $X = 1$
q = Reduced pressure $q = [1 - \exp(-\alpha p)]/\alpha$ (Pa)
$\dot{q}$ = Heat flux (J $m^{-2}s^{-1}$)
$\hat{q}$ = Integrated mass flow rate (kg s^{-1})
R_x = Reduced radius of curvature, $R_x = \left(\frac{1}{R_{x1}} + \frac{1}{R_{x2}}\right)^{-1}$ (m)
R_y = Reduced radius of curvature, $R_y = \left(\frac{1}{R_{y1}} + \frac{1}{R_{y2}}\right)^{-1}$ (m)
r = Relative film thickness $r = \frac{\bar{h}}{h_{cff}\,\bar{\rho}_c}$
r_a = Amplitude of waviness (m)
r_0 = Relative film thickness at $n = 0$
S = Sliding-to-rolling ratio, $S = (u_2 - u_1)/\bar{u}$
S = Surface of computational domain [m^2]
S_o = Sliding-to-rolling ratio in the center of the contact, $S = (u_2 - u_1)/\bar{u}$
s_0 = Viscosity-temperature index
T = Temperature (K)
T = Temperature rise in shear thinning analysis (K)
T_c = Temperature in the center of the film (C)
T_g = Glass transition temperature (K)
T_s = Surface temperature (C)
ΔT_s = Surface temperature increase (C)
T_0 = Initial oil temperature or reference temperature (K)
T_0 = Slotte equation constant (oil constant) (C)
t = Time (s)
$\bar{u}$ = Mean velocity, $\bar{u} = (u_1 + u_2)/2$ [m s^{-1}]
u_s = Slip velocity [m s^{-1}]
u_s = Sum velocity, $u_s = u_1 + u_2$ [m s^{-1}]
v = Elastic displacement (m)
v_f = Final elastic displacement, $v_f = v + v_h$ (m)
v_h = Hertzian elastic displacement (m)
w = Load per unit width [N/m]
X = Dimensionless coordinate $X = x/a$
x = Rolling direction coordinate (m)
y = Transverse direction coordinate (m)
z = Pressure viscosity index
α = Pressure-viscosity coefficient [Pa^{-1}]
γ = Starvation parameter
$\dot{\gamma}$ = Shear rate (s^{-1})
η = Lubricant viscosity (Pa s)
η_{bo} = Base oil viscosity (Pa s)
η_{cSt} = Lubricant viscosity in cSt [10^{-6} m^2s^{-1}]
η_{dim} = Dummy viscosity (Pa s)
η_g = Lubricant viscosity at glass transition temperature (Pa s)
η_0 = Lubricant viscosity at the contact inlet and ambient temperature (Pa s)
λ = Wavelength of a sinusoidal roughness (m)
κ = Ellipticity ratio $\kappa = \frac{a}{b}$
$\bar{\mu}$ = Jacod friction coefficient $\bar{\mu} = \frac{\mu_m p_o}{\tau_o}$
μ_m = Friction coefficient
ν = Poisson ratio
ρ = Density [kg/m^3]
$\bar{\rho}_c$ = Dimensionless density
ρ_o = Density at ambient pressure (kg/m^3)
σ = Internal stress in a body (Pa)
τ = Shear stress in the oil (Pa)
τ_L = Limiting shear stress value (Pa)
τ_y = Yield stress, grease (Pa)
τ_{y_0} = Yield stress at ambient pressure, grease (Pa)
τ_0 = Eyring shear stress characteriztic value (Pa)
ω = Angular frequency $\omega = 2\pi/\lambda$ (rad/m)

contact problem for grease lubrication. Later, in 1976, Hamrock and Dowson *(22)* solved the circular problem for oil lubrication. Their curve fit to numerical solutions is still the most widely used film thickness formula in EHL. Multilevel techniques were introduced by Lubrecht, et al. *(24)*, which made it possible in 1987 to numerically solve the equations with very dense grids, which increased the accuracy significantly. In the same year, Yang and Qiang *(26)* extended the work from Kauzlarich and Greenwood into grease lubricated elliptical contacts. Venner *(28)* further improved the numerical multigrid methodology and introduced the possibility of performing transient calculations using multilevel techniques. A comprehensive book has been written on multigrid methods in EHL by Venner and Lubrecht *(30)*. In 1994 Nijenbanning, et al. *(31)* introduced a new film thickness equation, based on a curve fit of these MultiGrid solutions. After 1994, there was no further need to improve the accuracy of the fully flooded film thickness formulae, and research in this area was directed toward starved EHL and non-smooth surfaces. For starved EHL, initially the same multigrid techniques were used (Chevalier, et al. *(32)*, refined by Damiens, et al. *(34)*). In 2008, Van Zoelen *(36)*, used a new approach based on thin film flow to solve this problem, making it possible to apply the formula to longer operating times and multiple contacts.

Mixed lubrication and the impact of roughness was studied using the full EHL equations (e.g., Zhu and Hu *(38)*). However, the concept of amplitude reduction (Venner and Lubrecht *(40)*) opened the possibilities to apply EHL theory to real surface roughness by means of a fast Fourier transform methodology (FFT; e.g. Morales-Espejel, et al. *(42)* and Masen, et al. *(44)*).

For a more extensive description on the history of EHL, the reader is referred to reviews by Spikes *(46)*, Dowson and Ehret *(47)* or Dowson *(1)*.

BASIC EQUATIONS

The Reynolds Equation

The general equations describing the motion of a fluid in space and time are the Navier-Stokes and continuity equations. The Navier-Stokes equations are derived using conservation of momentum and the lubricant is assumed to behave as a Newtonian fluid.

Usually, the inertia forces are assumed to be negligible, which simplifies the equations to the Stokes equations. Examples can be found in Odijk and Venner *(50)*, Almqvist and Larsson *(51)*, or Hartinger, et al. *(52)*. It is usually not necessary to solve the full equations. The narrow gap assumption (sometimes called the *lubrication assumption*), in EHL can be used to further simplify the equations leading to the Reynolds equation:

$$\frac{\partial}{\partial x}\left[\frac{\rho h^3}{\eta}\frac{\partial p}{\partial y}\right]+\frac{\partial}{\partial y}\left[\frac{\rho h^3}{\eta}\frac{\partial p}{\partial y}\right]=6u_s\frac{\partial(\rho h)}{\partial y}+6v_s\frac{\partial(\rho h)}{\partial y}+12\frac{\partial(\rho h)}{\partial t}. \quad [1]$$

The viscosity η and density ρ are a function of pressure. The film thickness is given by the original gap geometry (usually simplified to a parabolic shape) and the elastic deformation, d_e:

$$h(x,y)\approx h_0+\frac{x^2}{2R_x}+\frac{y^2}{2R_y}+d_e(x,y) \quad [2]$$

where $R_{x,y}$ is the reduced contact radii and h_0 is a constant.

Elastic Deformation and Film Thickness

In the case of dry contacts or severely starved contacts, the elastic deformation of the contact bodies can be described using the Hertz theory *(54)*. In the (well-)lubricated case this no longer holds. If the size of the contacting bodies is much larger than the size of the Hertzian contacts, plain strain prevails and the film thickness equation, including deformation, may be written as:

$$h(x,y)=h_0+\frac{x^2}{2R_x}+\frac{y^2}{2R_y}+\frac{2}{\pi E'}\iint_S\frac{p(x',y')dx'dy'}{\sqrt{(x-x')^2+(y-y')^2}}. \quad [3]$$

For more details on the elastic deformation the reader is referred to Johnson *(55)*.

The constant h_0 in Eq. [3] is the mutual distance of approach of two remote points in the bodies and may be solved using a force balance equation (Wijnant *(183)*):

$$m\frac{\partial^2 h_0}{\partial t^2}+\iint_S p(x,y)dxdy=F(t) \quad [4]$$

VISCOSITY–PRESSURE–TEMPERATURE RELATIONS

For the relation between viscosity and temperature at low pressure a number of models/equations exist. These can be classified into models based on fluid theory and on fitting measured viscosity at a number of temperatures. The temperature dependence of viscosity can be modeled by absolute reaction rate theory from the 1930s (Eyring *(57)*), described by, for example, Karis and Nagaraj *(58)* or Bogie and Harris *(60)*. However, more often simple equations, based on curve-fitting viscosity–temperature measurements, are used. These are listed by, among others, Crouch and Cameron *(122)*.

One of the most widely used equations is the Walther equation (e.g., Sánchez-Rubio, et al. *(63)*):

$$\log_{10}\log_{10}(\nu_{cSt}+a)=K-c\log_{10}T \quad [5]$$

This equation is the basis for the ASTM, ISO, and Deutsche Industrial Normale (DIN) charts and guidelines. For lubricating oils, a can be chosen as $a=0.8$ (Seeton *(64)*). The constants c and K can be calculated from the viscosity at two temperatures.

In EHL contacts, pressures are typically 1–3 GPa. This has a significant effect on the viscosity of the lubricant and therefore on the prediction of the lubricant film thickness and friction. Several equations for this are available where, unfortunately, the more accurate ones are also more complex and require specific viscosity measurement data. The simplest and most widely used equation is the Barus *(65)* viscosity pressure relation :

$$\eta(p)=\eta_0\exp(\alpha p) \quad [6]$$

where η_0 = viscosity at ambient pressure and α = pressure–viscosity coefficient.

For lubricating oils these variables will be approximately

$$0.001\le\eta_0\le 0.1\ \text{Pa}\cdot\text{s}$$

$$0\le\alpha\le 4.0\cdot 10^{-8}\ \text{Pa}^{-1}.$$

Unfortunately, the Barus relation predicts viscosities that are too high at high pressures.

A more accurate relation was proposed by Roelands *(68)* :

$$\eta(p, T) = \eta_0 \exp\left[\{\ln(\eta_0) + 9.67\}\left\{\left(1 + \frac{p}{p_r}\right)^z \left(\frac{T_0 - 138}{T - 138}\right)^{s_0} - 1\right\}\right] \quad [7]$$

with $p_r = 1.962 \times 10^8$ Pa; T_0 = temperature at which η_0 has been measured (K); s_0 = viscosity–temperature index, typically $1.0 \leq s_o \leq 1.5$, and z = pressure–viscosity index, typically $0 \leq z \leq 0.8$. By defining α as

$$\alpha = \frac{1}{\eta}\left(\frac{\partial \eta}{\partial p}\right)_{p=0, T=T_0}$$

the relation between z, α, η_0 reads:

$$z = \frac{p_r \alpha}{\ln\left(\frac{\eta_0}{\eta_{dim}}\right) + 9.67}, \quad [8]$$

where $\eta_{dim} = 1$ Pa·s.

For comparison, take a low loaded EHL contact with a pressure of approximately 0.5 GPa. Using an oil with viscosity $\eta_0 = 0.009$ Pa · s and $\alpha = 2.0 \times 10^{-8}$ Pa^{-1}, Barus's relation predicts a viscosity $\eta = 198$ Pa·s, whereas Roelands' relation predicts a viscosity $\eta = 46$ Pa·s.

Bair *(69)* has shown that the Roelands relation underestimates the viscosity at higher temperatures and suggests an equation based on free volume theory (Yasutomi, et al. *(71)*):

$$\eta = \eta_g \exp\left[\frac{-2.3 C_1 (T - T_g) F}{C_2 + (T - T_g) F}\right] \quad [9]$$

where η_g is the viscosity at the glass transition temperature ($O(10^7) < \eta_g < O(10^{12})$ Pa · s *(69)*. T_g is the glass temperature:

$$T_g = T_g(p = 0) + A_1 \ln(1 + A_2 p) \quad [10]$$

and the relative free volume expansivity is

$$F = 1 - B_1 \ln(1 + B_2 p) \quad [11]$$

and $A_1, A_2, B_1, B_2, C_1, C_2$ and T_{g0} are parameters to be fitted using measurements. As an example, for turbine oil T9, $\eta_g = 10^7$ Pa s, $T_g(p = 0) = -76°$C, $A_1 = 228.3°$C, $A_2 = 0.7645$ GPa^{-1}, $B_1 = 0.188$, $B_2 = 25.84$ GPa^{-1}, $C_1 = 11.45$, $C_2 = 30.26°$C. *(69)*, η_0(T = 40°C) = 0.0088 Pa s, and $z = 0.87$, $s_0 = 1.2$ (Liu *(72)*).

DENSITY, COMPRESSIBILITY

The lubricant density is a function of the size of the molecules from which it is composed and for a lubricating oil typically varies between 860 and 980 kg/m^3. The temperature dependence is usually neglected. For pressures below the solidification pressure, the variation of density with pressure is roughly linear up to a compression of approximately 35%. For pressures higher than the solidification pressure there is little change in density. A widely used formula describing this well is the Dowson and Higginson *(19)* density equation:

$$\rho = \rho_0 \frac{0.59 \cdot 10^9 + 1.34p}{0.59 \cdot 10^9 + p}. \quad [12]$$

The formula applies to both mineral and synthetic lubricants, except for silicones, for which compressibility is much higher than for mineral oils (Pirro and Wessol *(73)*).

NUMERICAL METHODS

The first numerical calculations to solve the equations listed above were done in 1976/1977 by Hamrock and Dowson *(22)*, *(74)*, *(75)* based on a simple Gauss-Seidel iteration scheme. They used these numerical calculations to derive their famous minimum and central film thickness equations, which are still widely used today. Others have further improved the method and extended the range of operating conditions and were able to achieve higher loads (e.g., Chittenden, et al. *(77)*, Evans and Snidle *(85, 86)*). In 1982 the Newton-Raphson method was introduced (Okamura *(90)*) to gain computing speed. In 1986 Lubrecht introduced multigrid techniques *(24, 94, 95)* that accelerated the computing process enormously. Later, Venner *(28, 93, 97, 99)* introduced a distributive relaxation scheme and a distributive line-relaxation scheme that made it possible to solve the EHL problem for high loads. Venner also introduced the multi-integration technique, developed by Lubrecht and Brandt *(100)*, into the multigrid solvers for EHL. Evans, Snidle and coworkers *(103)*, *(105)*, *(106)* have developed the so-called differential deflexion method, in which the main feature is an efficient calculation of the elastic displacements based on the half-space approach. This increase in efficiency and stability has allowed them to solve heavy-load, transient problems with real 3D roughness and also mixed lubrication cases *(107)*.

Computational fluid dynamics (CDF) techniques have been applied to solve the Navier-Stokes equations rather than the Reynolds equation *(51)*, Hartinger, et al. *(52)*. Here commercially available software can be used. However, although the results look promising, today only relatively low load cases can be solved with this technique.

Very recently, Habchi, et al. *(112)*, *(113)* have replaced the half-space approach used to solve for the elastic deformation in the film thickness equation (Eq. [3]) by full-body elasticity and managed to express the whole EHL formulation in a single system of equations that is solved in a iterative loop. This approach is known as the *full system approach* and has shown substantial benefits in dealing with heavy loads, thermal effects, and complex rheology in the lubricant (Habchi, et al. *(114)*, *(115)*. Currently, work is ongoing to solve the full Navier-Stokes equations with this technique.

ANALYTICAL METHODS FOR SMOOTH SURFACES

The main disadvantages of using numerical methods to solve the EHL problem are possible convergence issues and relatively high computing costs. Analytical solutions are preferred when many solutions are needed; for example, when multiple contact/transient problems need to be solved or for extensive parametric studies. To solve the problem analytically, engineers have simplified the problem, which made it not only possible to obtain solutions quickly but also led to a clearer understanding of isolated phenomena. Examples for smooth surfaces are the works of Ertel-Grubin *(10, 12)*, followed by many other authors; for example, Greenwood *(117)*, Greenwood, et al. *(119)*, and Christensen *(121)*, where simplifications are applied mainly to the geometry of the EHL contact, solving the inlet, center, and outlet regions separately. Recently a complete review of

these methods grouped under the name Ertel-Grubin has been presented (Morales-Espejel and Wemekamp *(124)*. Here only a short summary is given.

The Ertel-Grubin approach takes into consideration the following assumptions: the contact is infinitely long in the transverse direction (line contact), the lubricant follows Newtonian behavior and Barus's law (Eq. [6]), and the fluid is incompressible. The Reynolds equation applies, and the contact dimensions are small in comparison to those of the contacting bodies; thus half-space elasticity also applies. Introducing dimensionless groups (see Nomenclature), the Reynolds equation (Eq. [1]) becomes,

$$\frac{dQ}{dX} = K\frac{\hat{H} - \hat{H}^*}{\hat{H}^3}, \qquad [13]$$

where $\hat{H}^*$ is the film thickness value at the point where $dP/dX = 0$. The dimensionless pressure P can be calculated from the reduced dimensionless pressure Q,

$$P = -\frac{1}{K_1}\ln(1 - K_1 Q) \qquad [14]$$

where $K_1 = \alpha p_o$.

For the calculation of Q, Eq. [13] needs to be integrated,

$$Q = Q_s + K\int_{X=1}^{X} \frac{\hat{H} - \hat{H}^*}{\hat{H}^3} dX \qquad [15]$$

where Q_s is the value of Q at $X = 1$. The correct axis in the contact is X negative to the left of the contact center (inlet) and positive to the right; however, for simplicity of signs in the integrations at the inlet $-X$ will be replaced by X in the whole of this section; see Fig. 1. The calculation of the pressures Q and the film thickness $\hat{H}^*$ (originally at location $dP/dX = 0$, but under the assumption of parallel film, now at location $X = 1$ where $\hat{H}^* = \hat{H}_c$) can be done by imposing boundary conditions.

For the calculation of the reduced pressures, the Ertel-Grubin approach introduces the following assumption, $P \to \infty$ at $X = 1$, which becomes $q_s = 1/\alpha$ or $Q_s = 1/K_1$ at $X = 1$ *(12)*. This is a good approximation for any large P (not necessarily $P = \infty$).

Solution for $\hat{H}^*$

In the calculation of $\hat{H}^*$, the Ertel-Grubin approach introduces the following condition, $P = 0$ for $X = \infty$ (in a numerical scheme, this can be approximated to large values of X, namely $X = L$, with L being a sufficiently large number in order to avoid numerical starvation); substituting this in Eq. [15] and $Q_s = 1/K_1$ at $X = 1$, gives

$$0 = \frac{1}{K_1} - K\int_{X=1}^{\infty} \frac{\hat{H} - \hat{H}^*}{\hat{H}^3} dX \qquad [16]$$

At this stage Eq. [16] can be evaluated numerically for $\hat{H}^*$ (as originally done by Ertel-Grubin; see also Morales-Espejel, et al. *(42)*) using the Hertz shape for the inlet.

$$\hat{H} - \hat{H}^* = |X|\,(X^2 - 1)^2 - \ln\left[|X| + (X^2 - 1)^{1/2}\right] \qquad [17]$$

Moreover, a fully analytical solution for $\hat{H}^*$ and P is also possible by following the scheme of Wolveridge, et al. *(125)* (originally developed by Dowson and Higginson), with the use of Crook's remarkably accurate approximation for the inlet region close to the Hertzian zone,

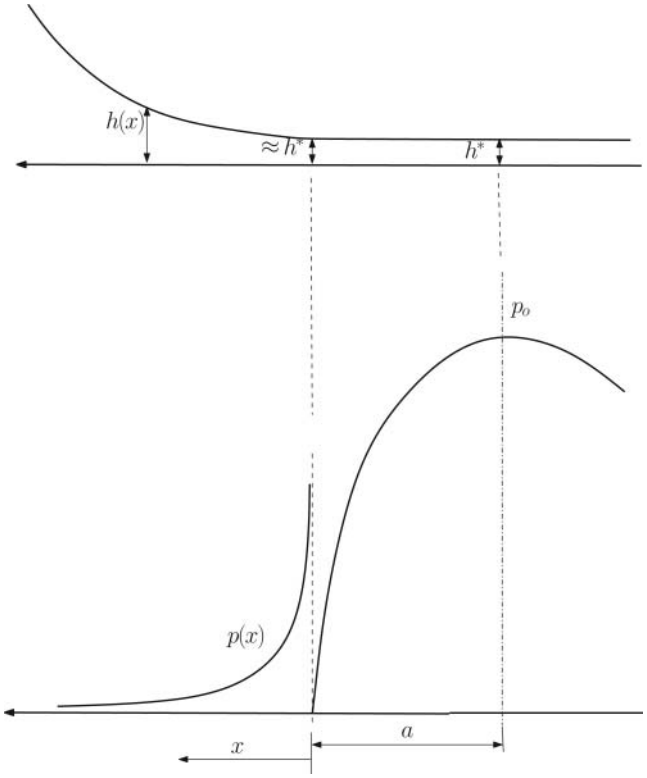

Fig. 1—Inlet geometry as considered by the Ertel-Grubin approach, given in dimensional quantities.

$$\hat{H}(X) = \hat{H}^* + C(X - 1)^{3/2} \qquad [18]$$

with $C = \frac{4\sqrt{2}}{3}$.

Substituting (18) into Eq. [16] and performing the integration (see Wolveridge, et al. *(125)*) yields

$$H^* = 0.2722\,(K_1 K)^{3/4} \qquad [19]$$

Solution for the Inlet Pressures

Once $\hat{H}^*$ is known, it can be substituted into Eq. [15] and the reduced pressures $Q(X)$ can be calculated numerically. Alternatively, K can be solved analytically from Eq. [16] and then substituted into Eq. [15]. Subsequently, Q can be transformed back into P by using Eq. [14], leading to:

$$P(X) = -\frac{1}{K_1}\ln[I(X)/I(L)], \qquad [20]$$

with $I(L)$ and $I(X)$ both given by Eq. [21] with different upper limits and with $\sigma = (X - 1)(C/\hat{H}^*)^{2/3}$.

$$I(X) = \frac{1}{(\hat{H}^*)^{4/3} C^{2/3}} \int_{\sigma=0}^{[(C/\hat{H}^*)^{2/3}(X-1)]} \frac{\sigma^{3/2}}{(1 + \sigma^{3/2})^3} d\sigma \qquad [21]$$

Off-Center Flat Solution from Greenwood

In the original publications of the Ertel-Grubin approach an attempt was made to calculate the location and the values of the outlet EHL pressure spike by using a combination of the pressures produced by a rigid-die contact and the Hertz solution

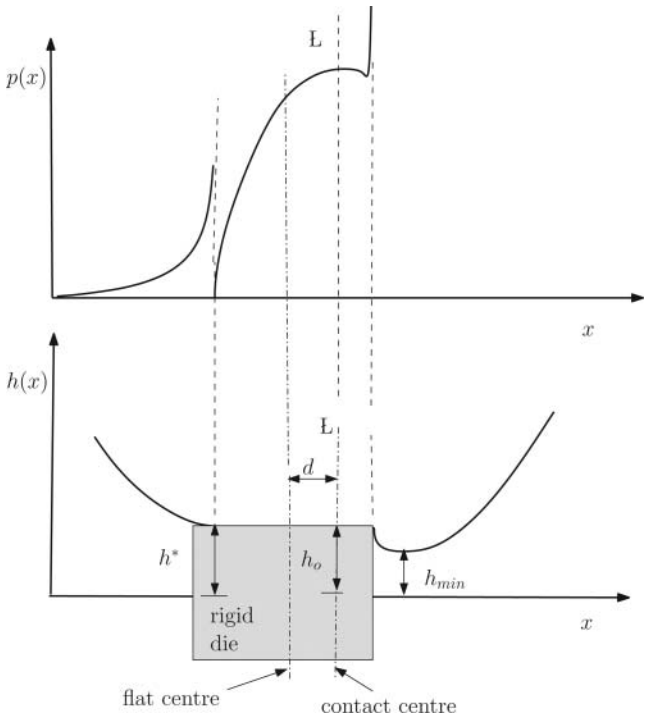

Fig. 2—Off-center geometry for the outlet Greenwood's solution.

(12). However, this attempt did not produce either minimum film thickness values or the exact location of the pressure spike.

Greenwood *(117)* introduced an extension of the Ertel-Grubin approach to calculate the left-hand side of the outlet pressure spike and the height of the outlet constriction, thus allowing for the calculation of the minimum film thickness in EHL contacts. The method is based on the assumption that the shape and pressures in this region can be approximated using the elastic solution of an off-center Hertzian flat, equivalent to an off-center rigid die; see Fig. 2.

Using linear elasticity solutions it is possible to calculate the pressure distribution in the central region and the elastic deformation outside the flat area. The Ertel-Grubin analysis for the inlet of the contact can be repeated here using the calculated inlet shape. This will produce the following equation:

$$\frac{a^2}{8\alpha\eta_o\bar{u}R_x^2} = 24\int_0^\infty \frac{A(\theta)\sinh\theta d\theta}{[H_o + A(\theta)]^3} \qquad [22]$$

where $A(\theta) = \sinh(2\theta) - 2\theta + 4(d/a)(\sinh\theta - \theta)$, $\xi = -\cosh\theta$, and $H_o = 4R_x h^*/a^2$. This integral can be evaluated numerically for given values of H_o and d/a.

Consider now the outlet, applying the Reynolds boundary condition (i.e., $q = 0$ when $h = h^*$) after the outlet constriction; therefore,

$$\frac{a^2}{8\alpha\eta_o\bar{u}R_x^2} = 24\int_0^{\theta^*} \frac{B(\theta)\sinh\theta d\theta}{[H_o - B(\theta)]^3} \qquad [23]$$

with $B(\theta) = 4(d/a)(\sinh\theta + \theta) - [\sinh(2\theta) - 2\theta]$ and θ^* is the value at which the film thickness returns to h^*, where $B(\theta^*) = 0$. Again, numerical evaluation is possible for given values of H_o and d/a. Finally, the solution of the problem provides to find these two constants for given operating conditions. This is achieved by iterations until the two integrals [22] and [23] are equated.

An important limitation of this approach is that the calculated outlet constriction does not consider the outlet hydrodynamic pressures (right-hand side of the pressure spike). Therefore, this might result in the prediction of slightly lower minimum film thicknesses.

Outlet Calculation—Complete EHL Solution

Greenwood and Morales-Espejel *(119)* and Morales-Espejel and Wemekamp *(124)* used the concept of linear fracture mechanics to develop an approach for the elastic displacement and pressure calculation in EHL contacts. This concept combined with the use of the Reynolds equation in a similar manner as used by Ertel-Grubin provides a method for the calculation of the inlet, central region, outlet geometries, and pressures in a complete EHL contact. Thus, the outlet hydrodynamic pressures can be calculated as well as their effects on the outlet shape. Complete line-contact EHL solutions can be obtained with this scheme. The approach has also been extended to (transient) variable-speed cases, (Morales-Espejel and Wemekamp *(124)*, and normal vibration problems Morales-Espejel *(126)*, with excellent agreement versus numerical solutions Félix Quinonez and Morales-Espejel *(127)*.

The only requirement for the application of elastic fracture mechanics equations is that in the cracked body the displacements along the line joining the crack tips should be zero. By considering a dry Hertzian contact it is possible to see that once the Hertzian deformation has occurred, any external traction applied outside the contact must produce zero displacements along the contact line. However, it will produce internal stresses $\sigma(x)$ similarly as a crack. Therefore, either a Hertzian or an EHL contact in this sense fulfills the conditions; see Fig. 3.

The final internal stresses $\sigma(x)$ in the body represent the final pressures in the EHL central zone of the contact, p_R is the outlet EHL pressures, and p_L is the inlet EHL pressures. Once the Herzian deformation has taken place, inlet $p_L(x)$ and outlet $p_R(x)$ pressures can be introduced and modified by iteration with the Reynolds equation (as done in the Ertel-Grubin scheme) to calculate the final elastic slopes produced by these pressures in their respective zones. Once the slope is calculated, it can be integrated to obtain the elastic displacements $v(x)$ produced by the inlet and outlet pressures. The final displacements are then obtained by adding the Hertzian displacements $v_h(x)$,

$$v_f(x) = v(x) + v_h(x) \qquad [24]$$

Greenwood and Morales-Espejel *(119)* includes some full examples reproduced here in Fig. 4, with the operating conditions given as Moes parameters *(153)*, *(152)*; M and L.

FILM THICKNESS MEASUREMENT TECHNIQUES

The current review article focuses on elastohydrodynamic lubrication theory; however, it is recognized that a large part of the theory; is either confirmed or inspired by experimental observations. Therefore, experimental aspects of EHL are briefly discussed in the present section. Comprehensive reviews on the topic (rheology, film thickness, pressures, temperature,

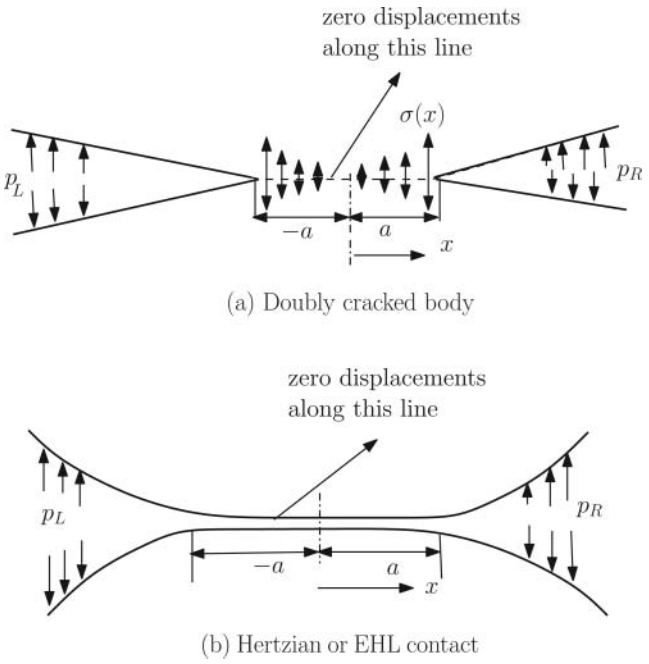

Fig. 3—Similitude in geometry between a doubly cracked body and a Hertzian or EHL contact.

and traction) can be found in, for example, Berthe and Vergne *(23)*, Spikes *(46)*, and Vergne *(179)*.

Parallel to the theoretical developments in the study of EHL contacts, important progress steps in the experimental techniques have occurred, particularly in optical interferometry for the measurement of film thickness, since its introduction by Gohar and Cameron *(96)*, *(98)*. Important improvements in this technique are due to developments in image analysis procedures, which give very accurate quantitative information from digitized interferograms in large regions of the contact (e.g., Gustafsson, et al. *(111)*; Molimard, et al. *(154)*, Krupta, et al. *(147)*). Another major improvement is the introduction of the spacer layer by Cann, et al. *(37)*, which allows the measurement of film thickness down to a few nanometers. Similarly, by using high-speed video cameras, Kaneta, et al. *(141)*, *(139)* showed that it is possible to study the full history of the passage of surface features under rolling/sliding conditions. Results from experimental techniques are extremely valuable because they are often used to verify the theoretical models. A nice example of this combined work is given by Félix Quiñonez *(87)*; see Fig. 5.

Today, the interferometry technique is the most accurate technique to measure film thickness. Its drawback is that one surface needs to be transparent, which does not represent the steel–steel surfaces that are usually found in, practice. For such contacts the electrical capacitance signal, being inversely proportional to the distance between the surfaces, may be used. Examples are given by Heemskerk, et al. *(123)* or later by Franke and Poll *(88)*, and Baly, et al. *(17)*. A recent development is the measurement of lubricating films between steel–steel surfaces through the reflection of an ultrasonic pulse (Dwyer-Joyce, et al. *(81)*). So far, these techniques are only applicable to relatively thick films (50 nm or larger).

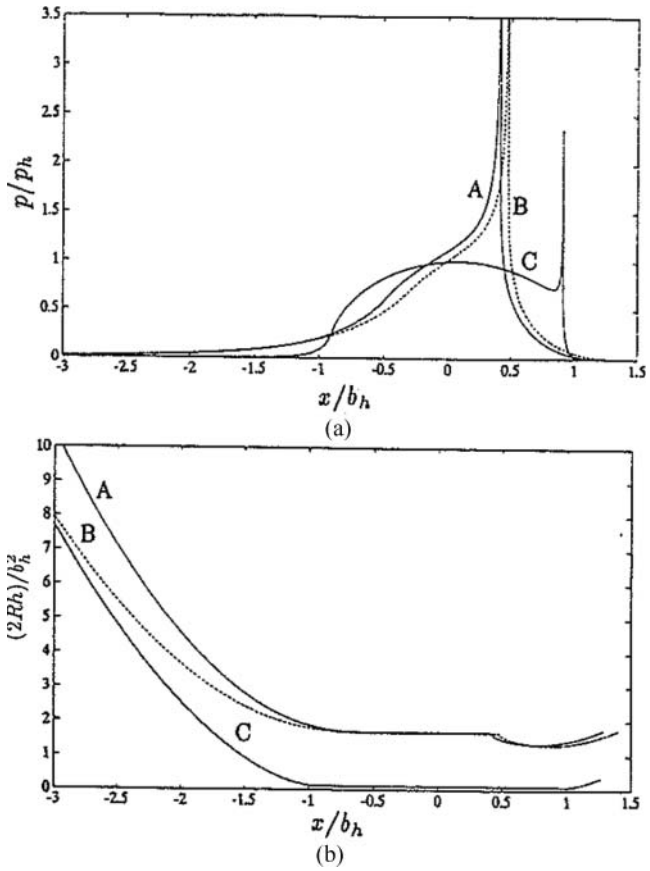

Fig. 4—Pressure distribution and elastic profile for a complete semi-analytical solution in EHL as given by Morales-Espejel *(155)*, with b_h = Hertzian semi-width, $p_h = p_o$. [A] – $M = 1057$, $L = 8.45$; [B] – $M = 1189.5$, $L = 8.45$; [C] – $M = 2469$, $L = 10.06$.

Some important work on temperature and pressure mapping can be found in, respectively, Reddyhoff, et al. *(167)* and Verge and Ville *(180)*.

THERMAL EFFECTS

Inlet Shear Heating

In general, the EHL films are only a fraction of a micrometer thick. This means that the volume of lubricant that is traveling through the contact is very small and that, provided that the contact is fully flooded, only a fraction of the lubricant can go through the contact clearance. Therefore, some of the lubricant close to the contact inlet will be rejected and will produce some reverse flow. This reverse flow shears the lubricant, generating heat that reduces the viscosity of the inlet lubricant, which again reduces the film thickness in the EHL contact (Cheng *(43)*). Greenwood and Kauzlarich *(102)* applied the hypothesis of Crook *(59)* that the principal mechanism of heat loss is conduction across the film and obtained a simple equation for a thermal correction factor for film thickness in line EHL contacts under pure rolling conditions and Newtonian fluid rheology:

$$\frac{h_{thermal}}{h_{isothermal}} \approx \left[1 - 0.240\frac{n\eta_0\bar{u}^2}{k(T_0 + T_s)}\right]^{3/4}, \qquad [25]$$

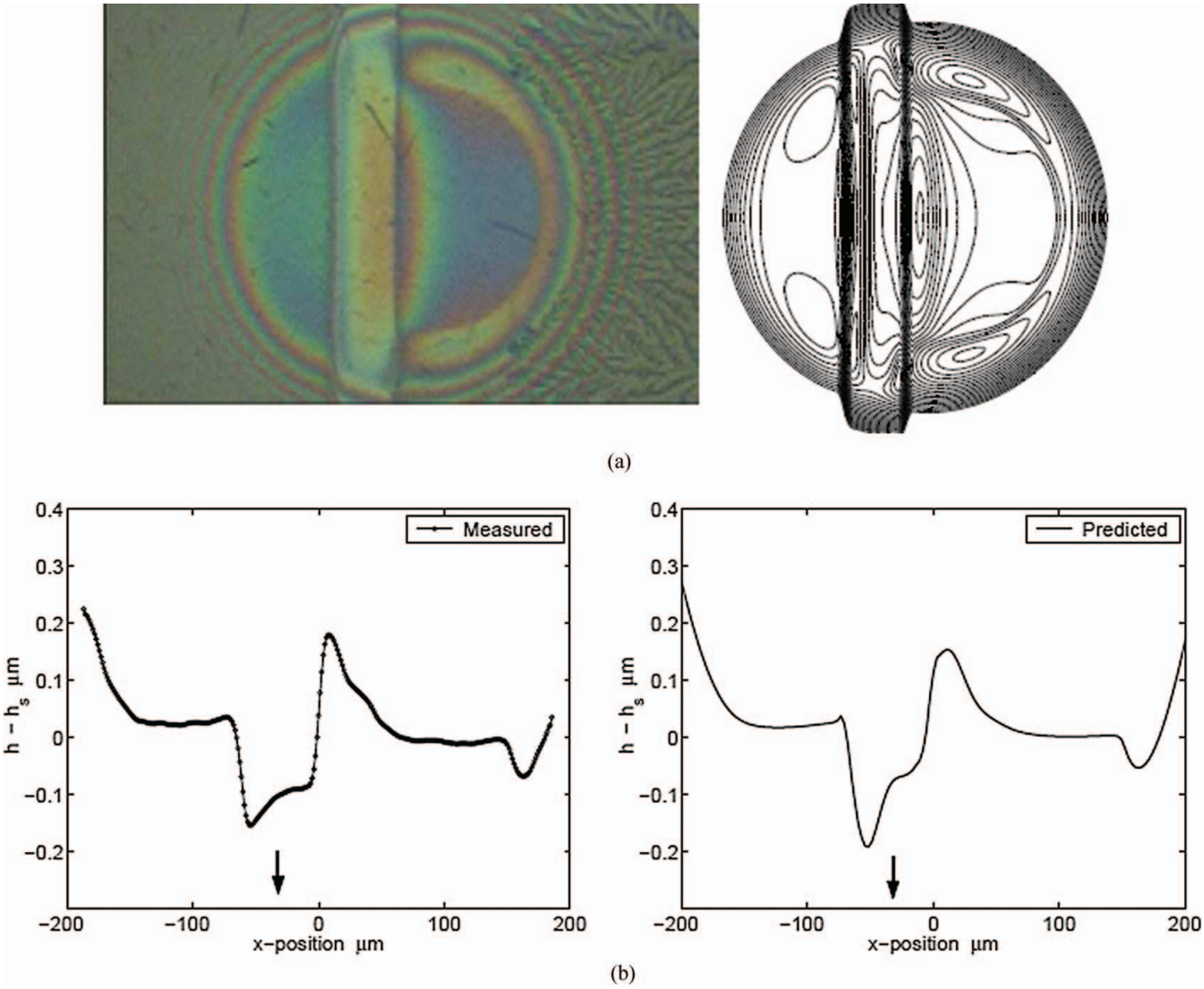

Fig. 5—Interferograms, contour maps of the predicted film thickness and corresponding experimental and numerical *x*-profile plots along $y = 0$ for a given time. Taken from Félix Quinonez *(87)*. The experiment was done under pure rolling conditions. N = Newtonian, NN = non-Newtonian simulations.

where the theory assumes that the viscosity of mineral oils depends on temperature and pressure according to a simple product rule,

$$\eta = \frac{A \exp(\alpha p)}{(T_0 + T_s)^n} \qquad [26]$$

with n, A, and T_0 being oil "constants".

The data from Cheng were later consolidated by Gupta, et al. *(110)* to produce an empirical formula for the film thickness thermal correction factor, which is also widely used.

Thermal EHL

Classical isothermal EHL theory generally considers Newtonian fluid and no temperature rise effects from sliding, which in the case of pure rolling may be sufficient for an accurate calculation of film thickness and inlet temperature rise (Greenwood and Kauzlarich *(102)*), but it certainly fails in the case of sliding in the contact, particularly when friction is being calculated. When sliding is considered in an EHL contact, a proper rheological model for the lubricant is essential as well as the consideration of the energy equation for the calculation of temperatures inside the lubricating film.

The interest in thermal effects for EHL lubrication first appeared with the theoretical work of Cheng *(45)*, *(41)*. Probably the first full numerical solution for the point contact problem was obtained by Zhu and Wen *(190)*. Since then, several authors have proposed different methods to deal with the thermal EHL problem assuming a Newtonian or a non-Newtonian lubricant, such as Kim and Sadeghi *(144)*, Guo et al. *(109)*, and Liu, et al. *(149)*, who solved the three-dimensional energy equation to determine the temperature variations throughout the lubricant film. An alternative method was proposed by Kim et al. *(143)*, who reduced the 3D heat transfer problem to a 2D one by assuming a parabolic distribution of the temperature across the film thickness. However, the parabolic temperature profile simplification leads to temperature predictions that may not be accurate at the inlet of

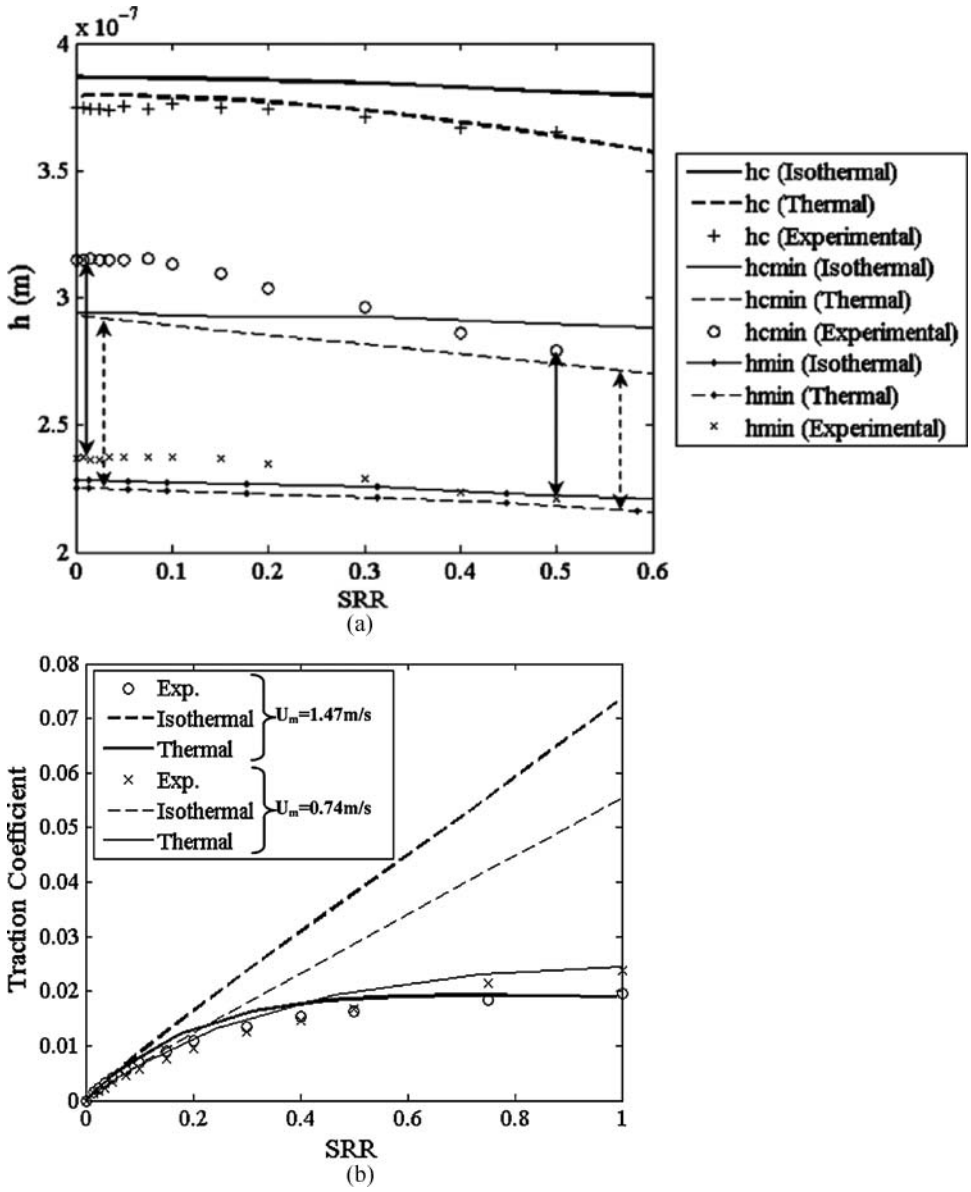

Fig. 6—Experimental and calculated film thickness and traction curves as a function of the rolling – sliding ratio for different entrainment speeds for Squalane + PIP (p_o = 0.47 GPa, $M = 30$ and $L = 7.8$). Taken from Habchi, et al. *(114).*

the contact, due to the complex thermal convective effects mentioned above.

In a full-system approach, Habchi, et al. *(114)* have obtained a complete resolution of the energy equation applied to both contacting solids and the lubricant film with the use of complex rheological equations for shear thinning and temperature effects. They compared calculations for film thickness and friction with measurements, and the results are summarized in Fig. 6

FRICTION AND SPIN

The prediction of friction in EHL contacts remains a challenge for engineers due to many unresolved issues. One of them is the understanding of rheological aspects of the lubricant in the conditions of an EHL contact, despite the progress already made. Another aspect is the friction caused by boundary layers providing the surface with lubricity, which substantially reduces typical dry-contact friction coefficients; that is, from 0.5 to 0.8 to more modest values in the order of 0.1 to 0.15. The properties of this layer and therefore its effects on friction depend largely on the chemistry of the lubricant–additive–surface system.

The final important aspect that considerably influences rolling and sliding friction in EHL contacts is the surface topography. Even in an ideal situation where all rheological and boundary layer aspects of the surface–lubricant couple are well–known, the calculation of the surface topography effects on friction is still a challenge. The greatest influence is generally found in the transition region from the boundary to full-film regime. However, in this section only cases of smooth surfaces will be discussed.

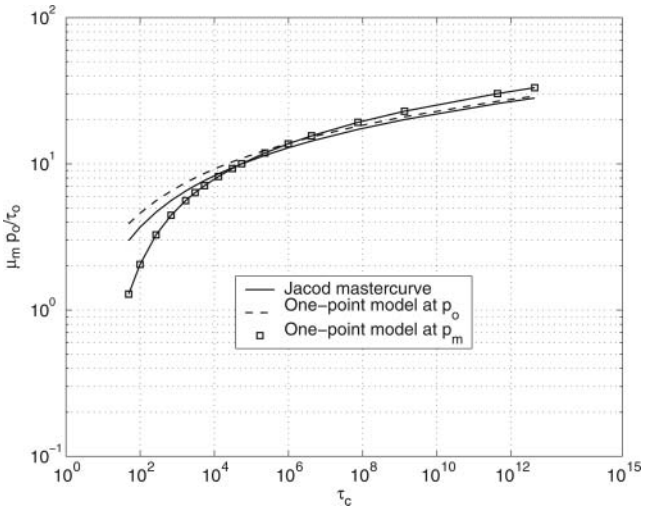

Fig. 7—Comparison of results after *(156)* for an Eyring fluid using Jacod's master curve, Jacod, et al *(134)*, the present one-point model Eq. [28] and the present one-point model with viscosity at p_o, Eq. [29]. where p_o is the maximum Hertzian pressure and p_m is the mean pressure in the contact.

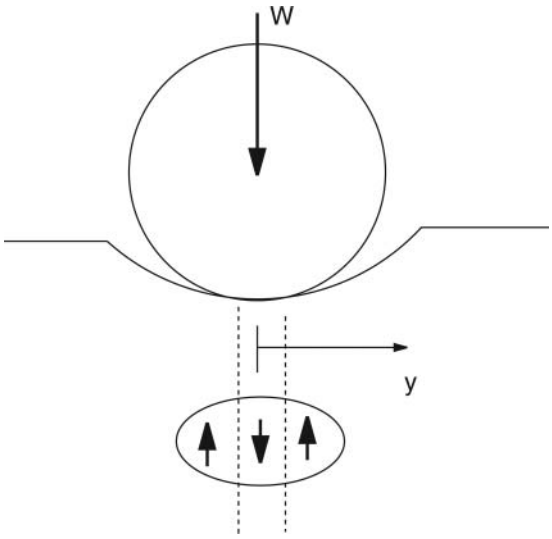

Fig. 8—Loaded ball rolling on a curved track. Below, the contact area showing two lines of pure rolling and zones of sliding.

Friction: Isothermal One-Point Model for an Eyring Fluid

Jacod, et al. *(134)*, *(135)*, *(132)* have reported "master curves" to predict the average friction coefficient for sliding elliptical and line EHL contacts with Eyring and limiting shear stress (LSS) fluids. The main conclusion of this analysis is that the traction force can be characterized by the conditions in the center of the contact. Therefore, the viscosity of the lubricant is evaluated at p_o and the geometry of the contact becomes irrelevant. Because this master curve is obtained from curve-fitting of full EHL numerical solutions, it implies that the contribution of the whole contact is included despite the fact that the parameters are calculated only in the contact center. The Jacod master curve for an Eyring fluid is

$$\bar{\mu} = \sinh^{-1}(\tau_c/5) \qquad [27]$$

where $\bar{\mu} = \mu_m p_o/\tau_o$ and τ_c, $\tau_c = \frac{2\bar{u}S\eta_{p_o}}{h_c\tau_o}$ with $\eta_{p_o} = \eta(p_o)$.

Morales-Espejel and Wemekamp *(156)* showed that similar behavior can be obtained by using a simplified one-point model, which is derived from a line-contact analysis across the film:

$$\bar{\mu} = \frac{\mu_m p_o}{\tau_o} = \frac{p_o}{p_m}\sinh^{-1}\left(\frac{\tau_c\eta_{p_m}}{2\eta_{p_o}}\right). \qquad [28]$$

This can be made equivalent to the Jacod master curve by choosing p_o instead of p_m; then

$$\bar{\mu} = \frac{\mu_m p_o}{\tau_o} = \sinh^{-1}\left(\frac{\tau_c}{2}\right) \qquad [29]$$

As shown in Fig. 7, this equation gives very similar results as Jacod's master curves.

From this figure it can be concluded that the master curve given by Jacod's model and Eq. [29] have the same physical roots. The only difference is the constant 5 in the argument of the $\sinh^{-1}$ function; for the one-point model this constant is 2 instead. The discrepancy is possibly due to the averaging effect of Jacod's model. It can be seen that the influence of this constant is mainly visible at very low sliding rates. This is probably due to the less accurate averaging effects of the latest methodology compared to Jacod.

Notice that despite the fact that Eq. [29] is a one-point model, it is a more reasonable model than the classical averaging method widely used to calculate mean friction coefficients, namely,

$$\mu_m \approx \tau_L/p_m = 3\tau_o/(2/3)p_o = 9\tau_o/(2p_o)$$

This equation when plotted in Fig. 7 would appear as a horizontal line at $\mu_m p_o/\tau_o = 4.5$.

Friction: Thermal Effects, Two-Dimensional Model

Again, following *(156)*, a simple two-dimensional thermal model can be obtained by assuming oil conduction only along the normal direction (e.g., Crook *(59)*). In this way, the integration of temperature-dependent viscosity in the contact area will be now possible. The domain is then discretized in $n_x \times n_y$ points, and for each grid point (i, j) a normal heat source can be calculated,

$$\dot{q}_{i,j} = \bar{u}S_{i,j}\tau_{i,j} \qquad [30]$$

Using the rheological model for an Eyring fluid, the shear stress matrix is

$$\tau_{i,j} = \tau_o \sinh^{-1}\left(\frac{\eta_{i,j}\dot{\gamma}_{i,j}}{\tau_o}\right) \qquad [31]$$

and for a limiting shear stress fluid,

$$\tau_{i,j} = \tau_{L_{i,j}}\left[1 + \left(\frac{\tau_{L_{i,j}}}{\eta_{i,j}\dot{\gamma}_{i,j}}\right)^n\right]^{-1/n} \qquad [32]$$

Notice that the limiting shear stress τ_L is considered in the reference as a variable quantity. The shear rate $\dot{\gamma}_{i,j}$ can also be a variable quantity if the slip profile is not constant in the contact (e.g., rolling bearings). The viscosity is function of pressure and temperature as given by Eq. [33].

$$\eta(p, T) = \eta_o f(p)g(T) \qquad [33]$$

To calculate the temperature rise distribution in the oil film, it is assumed that the heat vector is conducted only in the z direction, disregarding convection from the oil. The wall temperature rise ($(\Delta T_s)_{i,j}$) is calculated following an FFT procedure described in the reference *(156)*. This temperature is used as a boundary condition in a heat conduction analysis of a plate with internal heat generation (film) to calculate the lubricant temperature distribution. The following equation is obtained:

$$T_{i,j} = (\Delta T_s)_{i,j} + \frac{h\dot{q}_{i,j}}{12k_{oil}} \qquad [34]$$

An application example is included in the reference, where the sliding speed is allowed to vary in the contact area *(156)*. Consider the case of a loaded ball rolling on a curved track (ball bearing geometry) as shown in Fig. 10b. Macro-sliding will be induced due to the conformity of the contact. This configuration is similar to a ball-bearing ball running on its raceway.

For the described problem, in general the sliding velocity varies along the axis y, transverse to the rolling direction (along the longest semi-width b) following Eq. [35],

$$u_s(y) = S_o\bar{u}\left[1 - \left(\frac{y-c}{0.34b-c}\right)^2\right] \qquad [35]$$

where S_o is the sliding/roll ratio at the center of the contact, at $y = 0$, and c is an offset value of the center along y.

The same example of the ball bearing 6309, described in Houpert and Leenders *(130)*, is reproduced here, taking $c = 0$. The present 2D model was used to solve the described problem for increasing sliding velocity in the center of the contact.

Figure 9a shows the sliding velocity distribution in the contact, as obtained from Eq. [35] for the case in which $S_o = 0.0162$ (1.62 %) and $c = 0$. Figure 9b shows the corresponding distribution of surface temperature rise in the contact area for the fastest moving body with a mesh of 35×35 points, and low values of temperature rise are reached around the lines of pure rolling, where the heat input is relatively low. Figure 9c depicts the obtained temperature rise in the lubricant. The maximum value reached is 65°C and in the center of the contact the maximum is 32°C.

The results from the literature *(130)*, included in Fig. 9d show a maximum oil temperature of about 58°C and in the center ($y = 0$) the maximum value is about 26°C, read from the graph. The present calculations show the corresponding values of 60°C and 35°C, respectively. For the wall temperature, the reference *(156)* shows the two maxima at 8 and 4°C (from the graph), whereas with the present method the calculated values are 10.5 and 6.5°C; see Fig. 9b.

Friction: Spinning Effects

Relatively few publications deal with spinning effects on friction in EHL contacts. Most concern numerical studies. In the early days of numerical developments, Snidle and Archard *(168)* simulated a sphere spinning in a contact groove under hydrodynamic and pure spinning conditions. Later, Dowson and coworkers published several papers on this topic. Dowson, et al. *(78)* simulated the ball-on-plate contact under pure spin conditions; other papers are Dowson, et al. *(76)*, and Dowson and Xu *(79)*. Finally, Taniguchi, et al. *(171)* imposed rolling, sliding, and spin motions in elliptical contacts. More recently, Zou, et al. *(163)* and Yang and Cui *(157)* studied similar operating conditions. However, none of these papers treat friction; the focus is on pressure and film thickness only. Some publications in which friction in spinning contacts with thermal dissipation can be found are Tevaarwerk and Johnson *(172)* or, for isothermal conditions, Poon *(160)*. Here it is shown that spin motion decreases the friction-slip curve slope at low sliding-rolling ratio. A recent experimental study on rolling–sliding EHL contacts with spinning is from Dormois, et al. *(70)*. They also published work on a numerical study under isothermal conditions *(67)*.

Numerical simulations confirm the effect described by Tevaarwerk and Johnson that spin motion influences the initial slope of the friction curves. Consider, for instance, the geometry description as used in *(67)*, shown in Fig. 10a. The angle λ represents the amount of spin introduced in the contact. At large values (the limit is 90°) spin is reduced and at small values (the limit is 0°) spin is increased. Due to the rolling–sliding conditions introduced by both bodies, the disc and the spherical pin, the overall motion can be decomposed into three different parts, as shown in Fig. 10b: the entrainment speed, and the transverse, and longitudinal components of spin.

In the reference *(67)*, traction curves obtained from simulations are presented for different values of λ for the longitudinal and transverse friction coefficient. They are reproduced here in Fig. 11. The experimental results shown in *(70)* have the same tendency as Fig. 11a.

Non-Newtonian Effects on Film Thickness

A comprehensive review on rheological models for lubricants under high pressure is described given by Bair *(16)*. In general it is accepted that in a smooth-surface EHL contact, in the absence of sliding, the lubricant can be considered as Newtonian. However, in most applications, such conditions do not occur. Therefore the non-Newtonian behavior of the lubricant cannot be easily neglected and it is certainly imperative in the case of friction calculations. Some early numerical solutions of the EHL problem that considered a non-Newtonian model of the lubricant are from Gecim and Winer *(91)*, and Jacobson and Hamrock *(131)*. These studies considered a simple limiting shear stress model, which modified locally the Newtonian behavior by adjusting the lubricant velocity to accommodate the limiting shear stress.

Later, more sophisticated numerical models considering thermal effects appeared; for example, Wang, et al. *(181)*, Kim and Sadeghi *(144)*, Kim, et al. *(143)*, Guo, et al. *(109)*, Liu, et al. *(149)*, and Habchi, et al. *(114)*. In this last publication, comparisons between film thickness and pressures calculated with a Newtonian and a non-Newtonian model are shown. The results depict what is well known, a non-Newtonian lubricant tends to lower the pressure distribution and the pressure spike while having very little effect on the film thickness. However, friction is greatly modified.

Recently, Habchi, et al. *(115)* included the temperature and pressure dependance of some lubricant properties in their model. They used a single-Newtonian modified Carreau-Yasuda

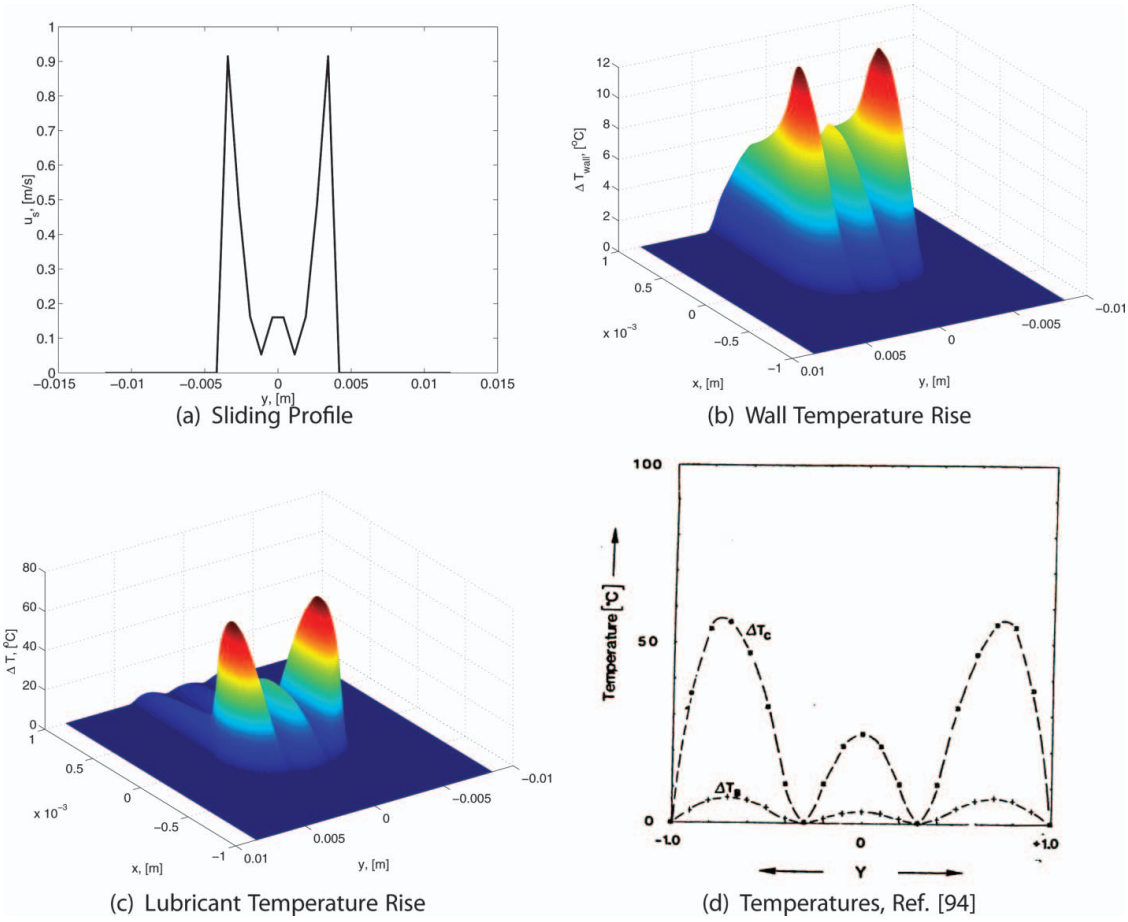

Fig. 9—Results taken from *(156)* Morales-Espejel and Wemekamp (a) Absolute sliding velocity profile in the contact across *y*, at $x = 0$ for the case of $S_D = 1.62\%$; (b) surface temperature rise distribution; (c) Lubricant temperature distribution, calculated with a mesh of 32 x 32 points; (d) Lubricant (ΔT_c) and wall (ΔT_s) temperature rise distribution as given by Houpert Lenders *(130)*.

rheology. Moreover, they made the conductivity and heat capacity of the lubricant temperature and pressure dependent. A comparison between model and experiment for film thickness and friction is shown in Fig. 12.

Figure 12a shows clearly that when it comes to film thickness predictions an isothermal non-Newtonian model can be very good. However, Fig. 12b shows a large difference between the predicted friction values. The thermal model with variable conductivity and heat capacity in the lubricant provided the best comparison with the experimental results.

STARVATION

The film thickness in a starved lubricated EHL contact is not only determined by contact geometry, speed, and lubricant physical properties but also by the lubricant supply to the contact. In the case that the contact is fully flooded, the pressure buildup starts relatively far upstream and with a near-zero pressure gradient, as shown in the left picture in Fig. 13. If the inlet is not fully filled, the contacting bodies contain two layers of oil, which merge and form a meniscus in the inlet of the contact and the pressure buildup can only start at this point; that is, closer to the Hertzian contact with a non-zero pressure gradient. The reduction in lubricant feed will reduce the film thickness and the shape of the characteriztic pressure distribution in the contact (see right side of Fig. 13). By reducing the lubricant supply further, the film thickness will continually decrease where the film will ultimately be equal to the oil layer supplied to the contact, compressed to about 30% by the high pressures. Sometimes starved lubrication is called *parched lubrication* (Kingsbury *(145)*).

The onset of starvation can be shown experimentally using optical interferometry measurements of a ball running on a glass disc lubricated by a thin layer of oil only. Pioneers in identifying and defining starved lubrication using these techniques were Wedeven, et al. *(182)*, Chiu *(53)* and Pemberton and Cameron *(159)*.

Figure 14 shows two interferometry images of ball-on-disc experiments. The colors indicate the film thickness and the lubricant flow direction is from the bottom to the top. The first picture was taken at relatively low speed, where there was enough time for replenishment and the second at relatively high speed where starvation occurs. In the low-speed case, Fig. 14a, the contact is almost fully flooded. Here the inlet meniscus at the bottom of the picture is far away from the edge of the Hertzian contact. At

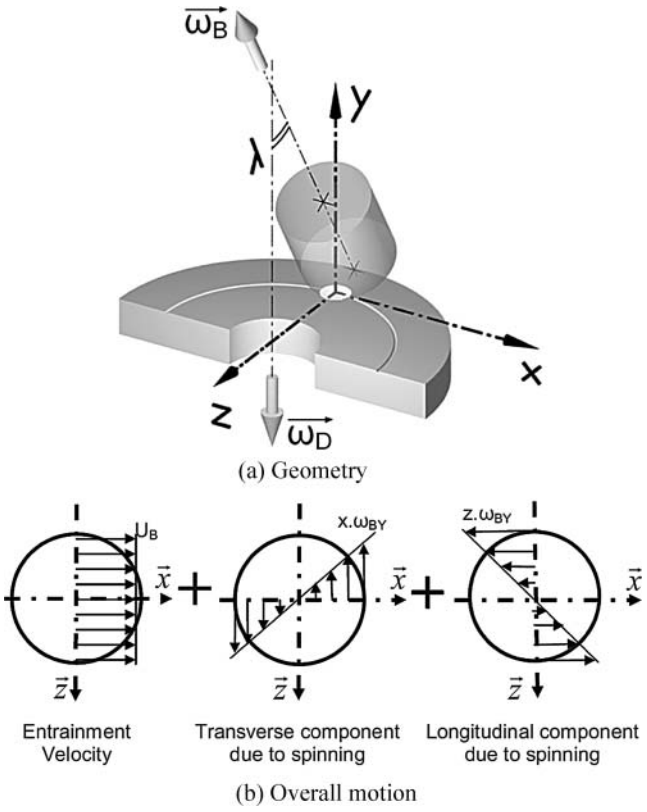

Fig. 10—Geometrical configuration and motion decomposition for a rolling–sliding–spinning contact, taken from Dormois, et al. *(67)*.

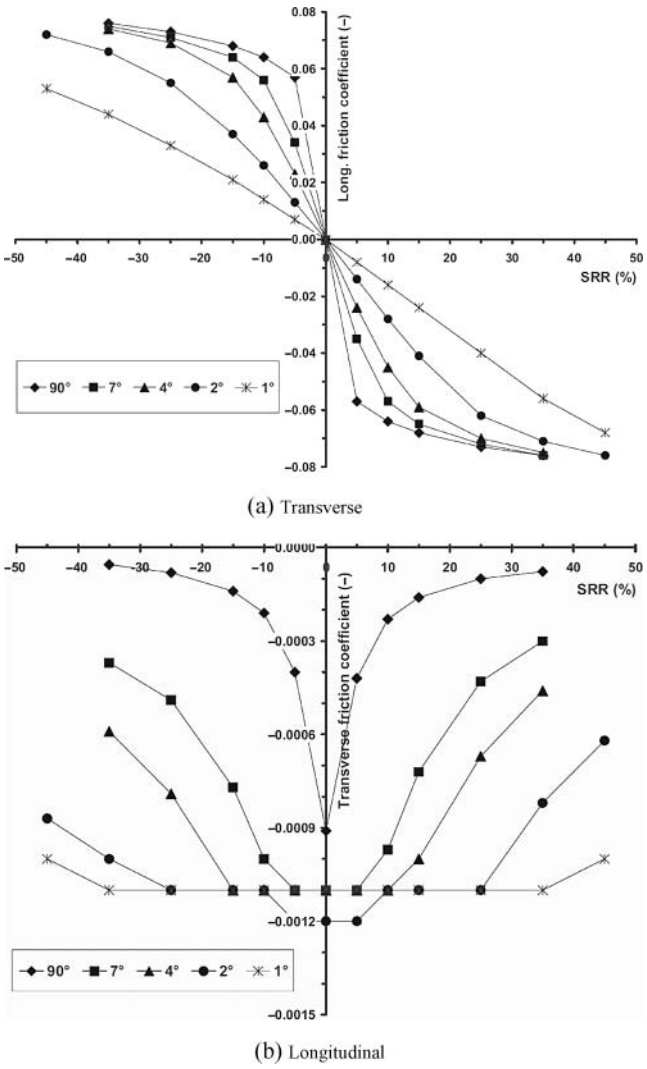

Fig. 11—Calculations results from Dormois, et al. *(67)* for the (a) longitudinal and (b) transverse friction coefficients versus sliding-rolling ratio for varying tilting angles.

higher speed, the inlet meniscus is hardly visible and the contact is severely starved.

In the starved lubrication regime, the film thickness is no longer accurately predicted by the Dowson and Higginson *(118)* or Nijenbanning *(31)* equations.

In 1971 Wolveridge, et al. *(185)* established a film thickness equation for starved contacts through a relation between inlet meniscus position and film thickness reduction for line contacts, followed by Hamrock and Dowson *(116)* in 1977 for point contacts. For engineering purposes, this is an inconvenient approach, because the inlet meniscus position is not a practical input parameter.

Chevalier *(48)* and Wijnant *(183)* used a different approach by assuming a layer of oil on the contacting surfaces with specified thickness $\tilde{h}$. In their numerical model the location of the inlet meniscus is then determined automatically by the continuity condition.

Mild Starvation

Chevalier, et al. *(32)* and Damiens, et al. *(34)* have done a large number of calculations on starved EHL contacts and derived through curve-fitting simple expressions for the film thickness in circular and elliptical contacts as a function of the inlet oil layer thickness:

$$\frac{h_c}{h_{cff}} = \frac{r}{\sqrt[\gamma]{1+r^{\gamma}}}, \qquad [36]$$

with

$$r = \frac{\tilde{h}}{h_{cff}\,\bar{\rho}_c}, \qquad [37]$$

where h_c = central film thickness; h_{cff} = central film thickness in case of fully flooded conditions (*(31, 118)*); $\tilde{h}$ = combined thickness of the oil layers in the inlet of the contact; and $\bar{\rho}_c$ = ratio of density at maximum Hertzian pressure and density under atmospheric pressure.

The parameter γ, representing the resistance to side flow, was found to be determined by a single nondimensional parameter representing the inlet length; see Fig. 15.

The experiments on ball-on-disc devices can be simulated by calculating the film thickness after repeated overrolling. The outlet film thickness h can be used as inlet layer $\tilde{h}$ for the next overrolling (corrected for compressibility). Damiens, et al. *(34)* have done this for 50 overrollings and found a relation for continuous

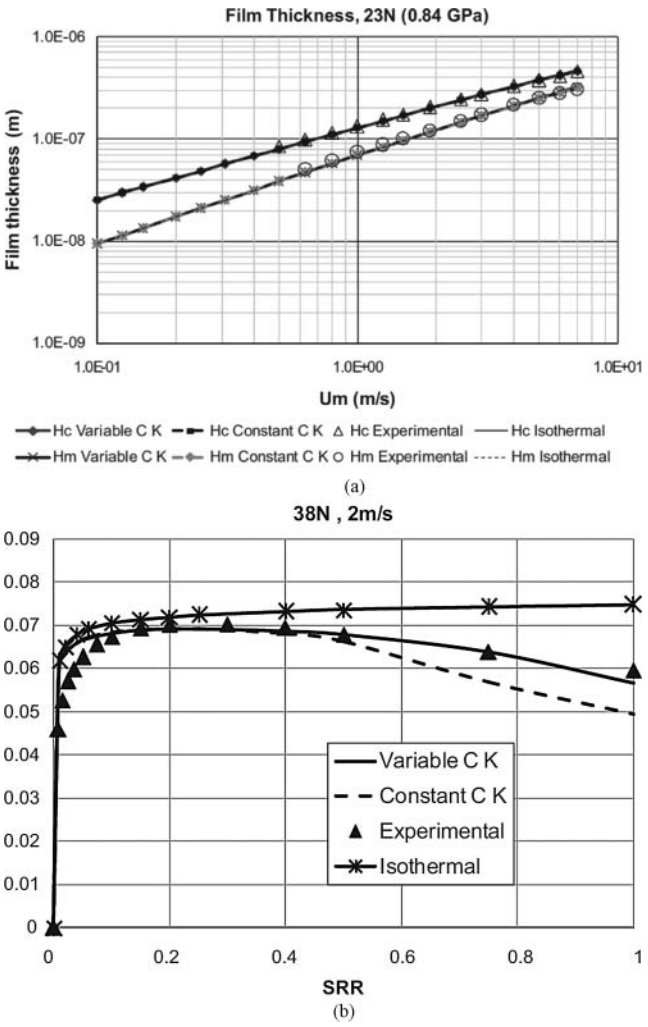

Fig. 12—Thermal non-Newtonian calculation and experimental results from Habchi et al. *(115)* for the (a) central and minimum film thickness in a steel-sapphire contact (b) traction curve in a steel–steel contact. The models used are: Isothermal, thermal with variable conductivity and heat capacity and thermal with constant conductivity and heat capacity. The contact maximum Hertzian pressure is 0.85 GPa.

overrolling:

$$\lim_{n\to\infty}\frac{h_c}{h_{ff}}=\lim_{n\to\infty}\frac{1}{\sqrt[\gamma]{1/r_0^{\gamma}+n}}\propto n^{-\frac{1}{\gamma}}. \qquad [38]$$

For a constant speed n, the film thickness decreases with time according to Eq. [38] and reads:

$$h_c(t)\propto t^{-1/\gamma} \qquad [39]$$

Severe Starvation

In the case of severe starvation, the inlet length will be very small and difficult to capture accurately on a numerical mesh. Therefore, as Damiens *(62)* pointed out, the numerically obtained results for γ are not as good for very thin films. Van Zoelen, et al. *(36)* have developed an analytical solution for this that gives more accurate results.

In the case of severe starvation, the pressure distribution can be approximated by the dry contact solution according to Hertz. The *film* thickness will be equal to the combined *layer* thickness feeding the contacts, compressed by the contact pressure. So the film thickness will be about 10–30% of the layer thickness.

By neglecting replenishment, the reduction in film thickness is caused by side flow in the contact:

$$\hat{q}_y(y,t)=\int_{-a(y)}^{a(y)}-\frac{\rho h^3}{12\eta}\frac{\partial p}{\partial y}dx \qquad [40]$$

for which Van Zoelen developed an semi-analytical expression,

$$h_{cs}(t)=\frac{1}{\sqrt{C_2 t+1/h_{cs,0}^2}} \qquad [41]$$

with $h_{cs,0}=h_{cs}(t=0)$,

$$C_2=\frac{p_o a\bar{\rho}_c^2 C}{3\eta_0 l_t b^2} \qquad [42]$$

and with

$$C=\int_{-a}^{a}\left[\left(\frac{\rho_0}{\rho(p)}\right)^2\left(\frac{\eta_0}{\eta(p)}\right)\left(\frac{p_o}{p}\right)\right]dx, \qquad [43]$$

where

$$p=p_o\sqrt{1-\left(\frac{x}{a}\right)^2} \qquad [44]$$

Here $\bar{\rho}_c$ is the dimensionless density in the center of the contact and l_t is the length of the track.

The viscosity and density in Eq. [43] are a function of the contact pressure and can be calculated using Roelands' equation (7) and the Downson and Higginson's equation [12]. With these equations it is very simple to calculate the film thickness for a starved EHL contact (neglecting replenishment). In the case of a constant pressure, Eq. [43] needs to be evaluated only once to obtain the C for Eq. [42], which gives C_2 for equation (41).

For severe starvation, the impact of load, viscosity and speed on film thickness is different than for fully flooded lubrication. With increasing load C decreases, which results in a decrease of the rate at which the film reduces in time as well. Physically, this means that the side flow from the contact reduces with increasing load due to the rapid increase in viscosity by increasing pressure.

Also note that the velocity is absent in the equations, which makes the rate of starvation a function of time only. After all, for higher speeds, a fraction of the oil layer on the track may be visited more often, from which one would expect more side flow. However, the duration will be shorter, which reduces the side flow again. The effect of speed, viscosity, and pressure on film thickness for starved and fully flooded contacts is summarized in Table 1.

For an accurate prediction of the rate of starvation, the models from Damiens and Van Zoelen should be combined. In essence, both models show the same film thickness decay

$$h(t)\propto t^{-1/\gamma} \qquad [45]$$

At the onset of starvation, Damiens' model is preferred and the power γ will be approximately 3 for circular contacts and up to 15 for wide elliptical contacts. For very thin films, as is usually

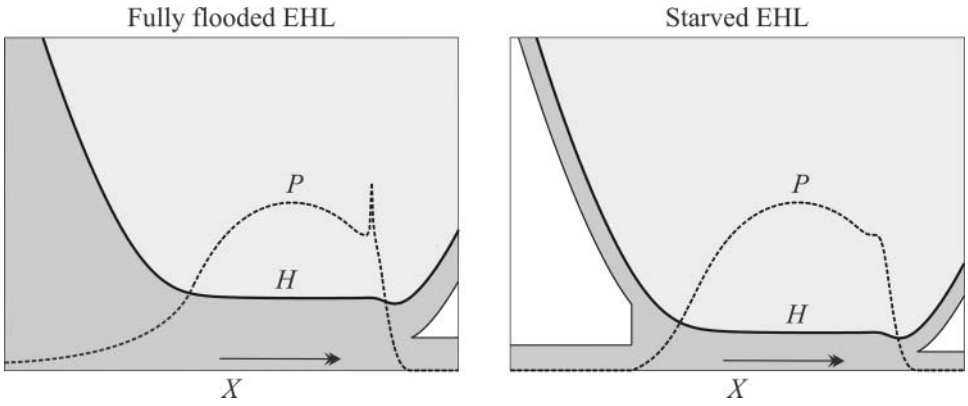

Fig. 13—Schematic representation of film thickness and pressure in a fully flooded and starved EHL contact (reproduced from Van Zoelen *(173)*, with permission).

the case in grease lubrication, Van Zoelen's model is preferred, which gives $\gamma = 2$ for all contacts.

Replenishment

As a result of the above-mentioned side flow, the layer thickness close to the centerline behind the contact will be thinner than that at the inlet side. However, lubricant that is pushed to the side may flow back into the track, generally referred to as *replenishment*. Figures 16a and 16b, from Åström, et al. *(11)* and from the authors's laboratory, show the typical butterfly shape of oil reservoirs that are formed for point contact in the case of limited oil supply and sufficiently high speed. The outlet layer thickness just behind the contact will approximately be equal to the film thickness corrected for compressibility (the oil may be compressed up to 30% in the contact and will "relax" back as soon as the pressure is relieved behind the contact). In front of the contact, part of the oil is pushed to the side (note that this will be less pronounced for wide contacts). Next to the track, two ridges, or side bands, are formed.

In the inlet of the contact some replenishment from the ridges may take place. Here the ridges are squeezed by the converging gap, causing some transverse flow and reducing starvation. Note that this is only significant for circular contacts, where these ridges are relatively close to the center of the running track.

Behind the contact the ridges may replenish the track due to, for instance, gravity and/or surface tension effects. Figure 16 represents a typical ball-on-disc situation where the disc ridges behind the contact may replenish the track within one disc revolution. In the absence of replenishment, the inlet layer thickness would be equal to the outlet layer thickness, which is clearly not the case in Fig. 16. The outlet layer width is larger than the inlet layer width, indicating that some replenishment occurred. Track replenishment was first modeled in 1974 by Chiu *(53)*, who assumed that the contact was fed by a uniform layer of lubricant. He solved the Stokes equation without any external force where the replenishment was driven by surface tension. Later, Jacod, et al. *(133)* included Van der Waals forces, which may be important for extremely thin films. Experimental visualization of the flow around an EHL contact was done by Pemberton and

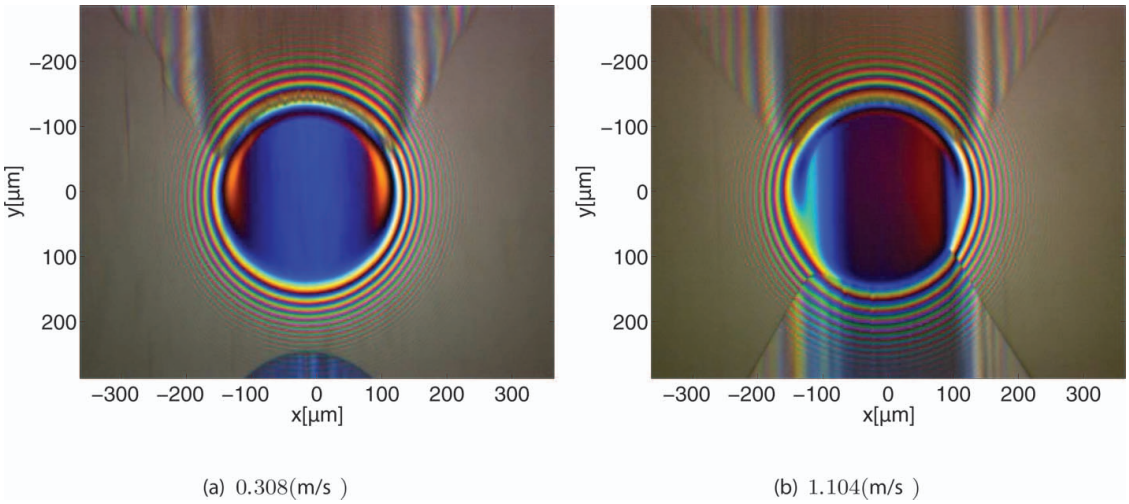

Fig. 14—Sequence of pictures taken from a interferometry film thickness measurement device showing the approach of the inlet meniscus of a starved EHL contact toward the Hertzian contact with increasing speed (reproduced from Popovici *(162)*).

TABLE 1—IMPACT OF SPEED, VISCOSITY, AND PRESSURE ON THE FILM THICKNESS AT A FIXED POINT IN TIME IN STARVED AND FULLY FLOODED EHL CONTACTS FOR WHICH THE CONTACT PRESSURE IS AT LEAST 0.1 GPA.

	Effect on Film Thickness	
Input	Starved (at Fixed Time)	Fully Flooded
$p \uparrow$	$h \uparrow$	$h \searrow$
$\eta_0 \uparrow$	$h \uparrow$	$h \uparrow$
$u \uparrow$	$h =$	$h \uparrow$

Increasing pressure leads to a large decrease in C (Eq. [43]), reducing C_2 in Eq. (42), which again reduced the film thickness according to Eq. 41. Increasing the base oil viscosity η_0 leads to a decrease in C_2 in Eq. [42], which loads to an increase in film thickness (Eq. [41]). Increasing the speed has no impact on the starved film thickness decay unless the initial film thickness $h_{cs,0}$ was equal to the fully flooded film thickness.

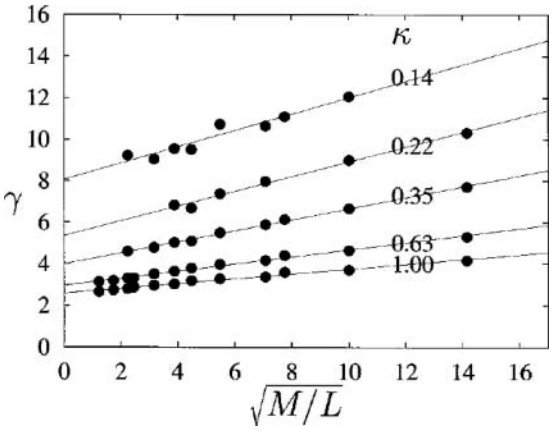

Fig. 15—Starvation parameter γ_c as a function of the Moes dimensionless numbers (M, L) and contact ellipticity κ (Damiens, et al. *(34)*). This is valid for $r = [0.5 : 1.5]$.

Cameron *(159)* using a very simple camera with a glass disc steel ball setup and showed two side bands of oil flowing around the contact that form a meniscus around the rear end of the contact. At higher speeds the two bands no longer merge and the meniscus is split into two side bands, similar to what can be seen in Fig. 16.

The formation of ridges was also observed by Guangteng and Spikes *(108)* in their experimental work. However, with the quantities of lubricant that Chiu *(53)* was using, they could only get starvation at very high speeds. This may be explained by the fact that the ridges were assumed to be infinitely wide in Chiu's model (so a uniform layer thickness outside the track).

Recently, thin film models have been developed by Gershuni, et al. *(92)* for flat surfaces and Van Zoelen, et al. *(174)* for axisymmetric rotating surfaces, where the Van der Waals forces have been neglected and are therefore only applicable for not too thin films ($h > 5$ nm). These models have been used to simulate the experiments from Fig. 17, which shows the replenishment of the ridges measured on a ball-on-disc experiment at the authors's laboratory. Gershuni found a good agreement between model and experiment, from which it may be concluded that Van der Waals forces can be neglected.

GREASE LUBRICATION

Lubricating grease consists of base oil, thickener material, and additives and shows a strong non-Newtonian rheology *(150)*. The film thickness in a grease-lubricated EHL contact will not be determined by the base oil only and the equations listed above often do not apply. In 1972 Poon *(161)* measured film thickness of grease in EHL contacts. He used a two-disc machine and measured the films using magnetic reluctance techniques and found films that are initially thicker than those expected based on the base oil viscosity only, followed by a decrease with time. Zhu and Neng *(191)* also measured the grease film thickness in line contacts and found that starvation was limited to a short initial period of about only one minute, after which the film thickness remained constant.

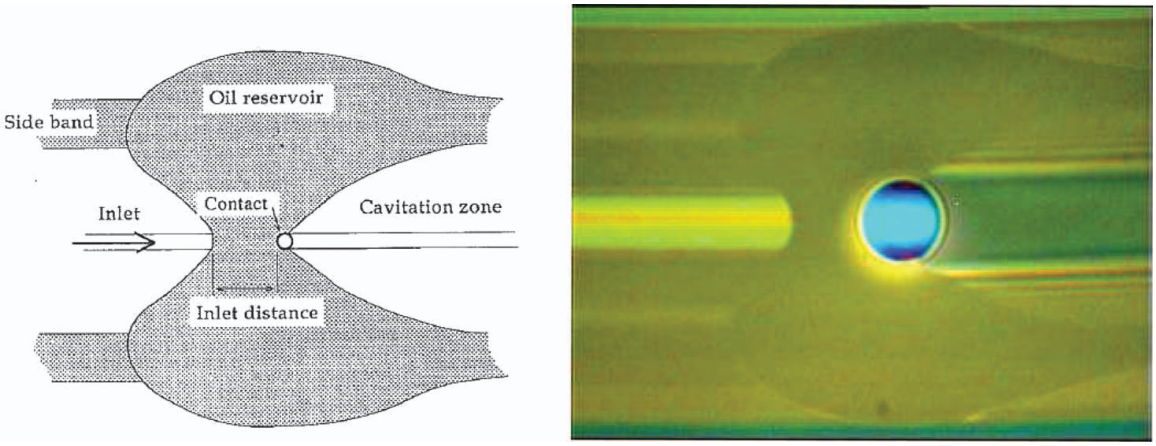

Fig. 16—The flow around an oil lubricated point contact at moderate speeds with limited oil supply (Åström, et al. *(11)* and the authors laboratory), showing side bands and oil reservoir. The contact is still fully flooded. Inlet on the left side of the figure.

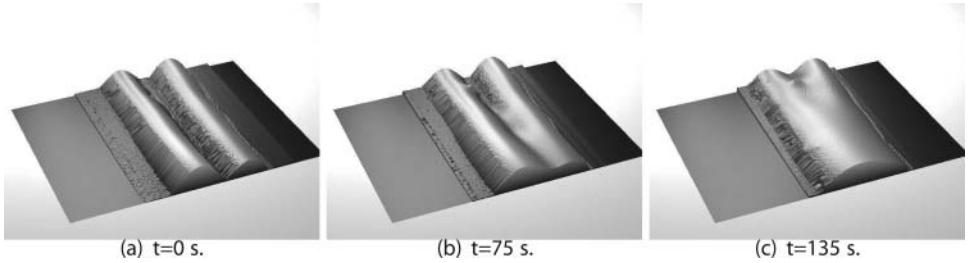

Fig. 17—Height measurement of the two layers formed behind the ball-on-disc contact for three moments in time (Gershuni, et al. *(92)*).

Later, when very accurate optical interferometry measurements on a ball-on-disc configuration became available, fully flooded measurements were done using a scoop to ensure fully flooded conditions. In this case, grease is continuously "pushed back" into the inlet of the contact and only a mild form of aging occurs. This makes it possible to measure during longer times with fresh grease. Such measurements have been done by Aström et al. *(8)*, Williamson, et al. *(184)*, Kaneta, et al. *(140)*, and others, who showed that the film thickness is indeed higher than the fully flooded oil film thickness. The optical setup also made it possible to show that grease thickener lumps were entering the contact.

Fully Flooded Grease-Lubricated Contacts

In the case that the EHL contact is fully flooded (with relatively fresh grease), as in the ball-on-disc measurements described above, the traditional Newtonian viscosity has to be replaced by non-Newtonian grease rheology. In 1972 Greenwood and Kauzlarich *(20)* derived an analytical expression for the 2D grease film using a Herschel-Bulkley model,

$$\tau = \tau_y + K\dot{\gamma}^n. \qquad [46]$$

Later, in 1979, Jonkisz and Krzemiński-Fredihave *(137)* numerically solved the line contact grease-EHL problem with the same Herschel-Bulkley model, obtaining a slightly more accurate solution compared to the Kauzlarich and Greenwood model.

In both papers, and also later in Bordenet, et al. *(25)* it was shown that in the inlet two layers exist: one layer where the shear stress exceeds the yield stress and where grease flows as a viscous liquid and a layer where the shear stress is smaller than the yield stress and where a plug flow occurs. This is illustrated in Fig. 18 for pure rolling.

The occurrence of a plug flow in the high-pressure zone of the EHL contact is obvious due to the exponential relation of the viscosity with pressure. In the inlet, viscous behavior is observed close to the wall and a plug flow will only occur in the center of the film. Further upstream, which is not shown in this figure, the pressure gradient will be so small that the velocity will again be constant across the film.

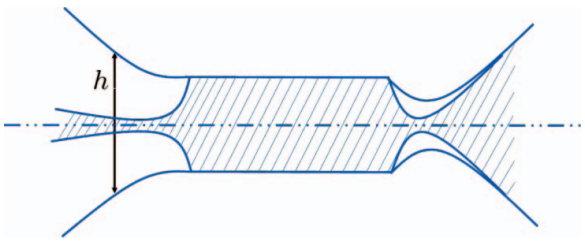

Fig. 18—Film profile *h* and plug flow in a grease lubricated pure rolling EHL contact.

For the prediction of the film thickness, Kauzlarich and Greenwood use the above-mentioned Grubin theory in EHL. Assuming an exponential relation for yield stress τ_y and consistency K, similar to what was done for base-oil viscosity, makes it possible to derive a film thickness equation for line contacts *(20)*:

$$h_c^{n+\frac{1}{3}} = \frac{2^{\frac{3}{2}}\pi^{\frac{1}{6}}}{3^{\frac{1}{3}}}\left(\frac{E'}{w}\right)^{\frac{1}{6}} R^{\frac{1}{2}}\alpha K_0 \bar{u}^n \left[\left(4+\frac{2}{n}\right)^n I(n) + \frac{\pi}{\sqrt{3}}\frac{\lambda_n \tau_{y_0} h_c^n}{K_0 \bar{u}^n}\right] \qquad [47]$$

with

$$K = K_0 \exp(\alpha p)$$
$$\tau_y = \tau_{y0} \exp(\alpha p)$$
$$I(n) = \frac{(n-\frac{1}{3})!\,(n-\frac{2}{3})!}{2\,(n!)} \qquad [48]$$
$$\lambda_1 = 1 - \frac{1}{3}\left(\frac{2z_p}{h}\right)^2 \qquad \frac{2n+1}{n+1} < \lambda_n < 1.$$

Here w is the load per unit width. The noninteger factorials in [48] can be calculated using

$$n! = \Gamma(n+1) = \int_0^\infty e^{-t} t^n dt. \qquad [49]$$

This means that $\frac{2}{3} < \lambda_1 < 1$. For bearing greases, $n \approx 0.3$, so $1 < \lambda < 1.25$ and $I(n) \approx 0$. Under practical conditions the last term in Eq. [47] is negligible. So the film formation is determined mainly by the consistency K_0 and speed. Kauzlarich and Greenwood also derived an equation for the inlet shear heating based on the same Herschel-Bulkley model:

$$T_c - T_s = \frac{2^{n-1}\left(2+\frac{1}{n}\right)^n}{3+\frac{1}{n}} \frac{K\,(\bar{u})^{n+1}}{k_{grease}} \frac{(h-h_c)^{n+1}}{h^{2n}}, \qquad [50]$$

where k_{grease} is the thermal conductivity of the grease. The film thickness Eq. [47] shows a power law behavior (plotting film thickness versus speed on logarithmic scales will give a straight line) between speed and film thickness.

A more appropriate grease rheology model was proposed by Bauer *(21)* where it was assumed that the grease viscosity approaches the base oil viscosity at high shear rates (see also Baart, et al. *(13)*):

$$\tau = \tau_y + \eta_{bo}\dot{\gamma} + K_2\,(\dot{\gamma})^n. \qquad [51]$$

Here η_{bo} is the base oil viscosity. In 1988, Dong and Qiang *(66)* developed a line contact model using this rheology and proposed the following film thickness formula:

$$\frac{h}{h_{oil}} = \left(1 + \Upsilon^{1.1}\left(\frac{h_{oil}}{R_x}\right)^{1-n}\right)^{0.69} \quad [52]$$

where

$$\Upsilon = \frac{\eta_{bo}}{K_2}\left(\frac{\bar{u}}{R_x}\right)^{n-1} \quad [53]$$

Again, as in the Kauzlarich and Greenwood equation [47], the correction for the film thickness does not contain the yield stress.

Bordenet, et al. *(25)* used the same rheology model but now for *point contacts*. Unfortunately, they did not give a film thickness formula. However, they also found that the base oil viscosity was the most important parameter here, that the yield stress does not have an impact on the film thickness, and that the films can be corrected using the consistency K_2.

Yang and Qian *(26)* argued that shear thinning can be neglected in grease-EHL contacts because the grease typically operates under high shear rates. They derived a 2D solution for elliptical contacts using the Bingham plastic rheology model (Eq. [46], with $n = 1$). They derived a relatively simple film thickness equation for fully flooded contacts:

$$\frac{h}{h_{oil}} = \left(\frac{K}{\eta_{b0}}\right)^{0.74}, \quad [54]$$

with K the Bingham grease viscosity.

Starved Grease-Lubricated Line Contacts

Single contact film thickness measurements from Zhu and Neng *(191)* showed that, for line contact, film thickness decay only occurs in the first minutes. After this a constant film thickness was measured. They ascribed this behavior to the Herschel-Bulkey rheology of grease. Transverse flow in the line contact inlet does not occur as long as the shear stresses are lower than the yield stress. Mechanical work on the grease (churning) will slowly reduce the yield stress, and at some point in time side flow in the inlet will occur. For line contacts the pressure gradient across the contact will be very small and the starvation rate $\frac{dh}{dt}$ will therefore also be small.

Starved Grease-Lubricated Point Contacts

Almost all measurements that can be found in the literature using optical interferometry in point contacts show that starvation occurs in the case of grease lubrication. Like with oil, recovery is sometimes reported due to replenishment of the track. Sometimes replenishment is ascribed to base oil replenishment. In many cases a more complex behavior is observed.

Merieux, et al. *(151)* classified grease film thickness (point contact) measurements according to their replenishment behavior into four categories:

- Fully flooded
- Starved
- Starved with stabilization
- Starved with recovery

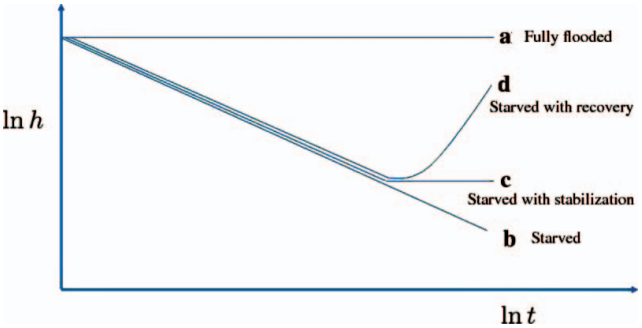

Fig. 19—Characteriztic starvation behavior for grease lubrication (reproduced from Merieux, et al. *(151)*).

This is schematically shown in Fig. 19.

Merieux et al. claimed that lubrication behavior *d* is caused by grease degradation in the edge of the contact. Grease is pushed to the side by overrolling and the small quantity that is just close enough to the Hertzian contact is sheared during each passage of the ball, causing mechanical aging of the grease. The grease is transformed from a Bingham plastic or Herschel-Bulkely-like material into a more viscous material.

To model this behavior they used a rheology model defined by Czarny and Moes *(61)*:

$$\tau = \left[\tau_y^n + (\eta\dot{\gamma})^n\right]^{1/n} \quad [55]$$

in combination with a shear degradation model:

$$\tau_y = \frac{\tau_o}{(1 + \dot{\gamma}t)^{\alpha}}. \quad [56]$$

Here τ_o is the initial yield stress, t is the time, and α a coefficient. The degradation of grease was calculated by assuming a simple velocity profile in the deformed Hertzian geometry, giving the shear rate as a function of time. Replenishment is assumed to occur when grease turns into oil, which is assumed to happen as soon as the yield stress has reached a value of $\tau_y = 40$ Pa. So the replenishment is assumed to depend on the grease shear stability. Couronné, et al. *(56)* assumed that contact replenishment for grease-lubricated point contacts is determined by the elastic modulus G' of the grease, which should be low. However, as in the paper by Merieux et al. *(151)*, the experimental evidence is very thin.

There are also strong indications that the grease-lubricated contacts are layered. Relatively thick boundary film layers formed by degraded thickener have been observed to occur in point contact film thickness measurements. This could explain behavior c in Fig. 19; that is, starvation ultimately leading to a stabilized film. Such measurements have been done by Cann *(33)*, who found that the grease film was composed of two parts: one that is formed by hydrodynamic action and the other formed by a residual layer:

$$h_T = h_R + h_{EHD}, \quad [57]$$

She found residual films with thickness 6 nm $< h_R <$ 80 nm. Grease films were chemically analyzed earlier by Cann and Spikes *(39)*, showing that significant amounts of thickener are

present on the track. It is presumed that this is deposited by grease as it is shear degraded in the contact.

SURFACE ROUGHNESS AND ANALYTICAL METHODS FOR MICRO-EHL

Waviness

Patir and Cheng *(158)* showed that transverse roughness improves the pressure flow and, as a result, film thickness. In their analysis, it is most important to note that no elastic deformation of the roughness was taken into account, which could only be included when modern algorithms were developed and fast computers became available for solving the full EHL problem. These techniques were used by Venner, et al. *(177)*. They showed that this positive effect of transverse roughness could not be observed in the case of fully flooded lubrication conditions. They performed calculations where the amplitude of the waviness was 0.08 μm under conditions where a smooth central film thickness of 0.12 μm could be expected (so $\lambda < 3$).

Figure 20b shows that the transverse waviness does not influence the average film thickness in time. In the case of sliding, the roughness does have an influence on the average film thickness. If the rough surface is moving faster than the smooth surface, an extra amount of oil is pumped in the contact and the average film thickness increases (Fig. 20c). If the rough surface is moving slower, then the effect is similar to pure rolling. Figures 20a, 20b, and Fig. 20c show the film thickness for transverse waviness entering the contact. For pure sliding Jeng *(136)* showed that longitudinal roughness gives higher friction in mixed lubrication than transverse roughness. He used a pin-on-disc machine where the rough surface was stationary loaded against a smooth rotating disc, so his results confirm the Patir and Cheng theory. Also, Ehret, et al. *(82)* found that the roughness layer should be transverse to the running direction, particularly when sliding is present in the contact. Measurements for film build–up and friction with various engineered surfaces can be found in Lugt et al. *(192)*.

An Analytical Method for Rough Surface EHL

To compute pressure and film thickness in real rough surfaces using numerical methods, a very dense grid is required, which makes computing times very long. This is even the case with the modern fast methods such as described above. An analytical solution/approximation is therefore strongly preferred. Greenwood and Johnson *(101)* first noticed that in EHL, sinusoidal roughness would produce nearly sinusoidal pressure ripples, and in the presence of sliding (with a Newtonian fluid), the roughness is largely flattened and replaced by large pressure ripples. They worked out simple relationships to describe pressure and deformed roughness. Venner *(28)* observed that at the center of a low-amplitude wavy EHL contact, the lubricant viscosity is so high that the Poiseuille flow term in the Reynolds equation can be disregarded. Reducing it to a simple linear transport equation gives

$$\bar{u}\frac{\partial(\rho h)}{\partial x} + \frac{\partial(\rho h)}{\partial t} = 0 \qquad [58]$$

Based on this very important observation, Greenwood and Morales-Espejel *(104)* developed a methodology for the calculation of pressures and deformation for any sinusoidal roughness. This methodology can easily be extended for any transverse roughness by decomposing it in Fourier terms.

Newtonian Fluid

The solution for micro-EHL pressure and local film fluctuations with transverse roughness in a line contact and with Newtonian fluid is described in reference *(104)* in detail. There, the complete transient solution of the problem is shown to be made of two components: (1) the particular integral; that is, steady-state solution of the problem, and (2) a complementary function; that is, flow excitation at the inlet of the contact produced by the incoming (partly deformed) roughness and solution of the homogeneous Eq. (58); see Fig. 21, where for clarity a case of rolling–sliding is shown. The reference *(104)* shows equations for the two solutions considering an initial sinusoidal roughness. However, the amplitude of the complementary function cannot be obtained with the original method of the reference *(104)*, because the inlet is not included in the formulation. Morales-Espejel, et al. *(42)* used the amplitude reduction numerical results from Venner and Lubrecht *(40)* to calculate this amplitude, because in Newtonian conditions the complementary function dominates the deformed clearance; this deformation is controlled by a new variable, ∇.

$$\nabla = (\lambda/a)M^{0.5}L^{-0.5} = \sqrt{\frac{\pi}{3}}\frac{\lambda p_0^{1/2}}{\sqrt{\eta_o \bar{u}\alpha}R_x^{1/8}E'^{1/4}} \qquad [59]$$

For 3D contacts and 3D micro-geometry, it is possible to extend the scheme by considering the central part of the contact

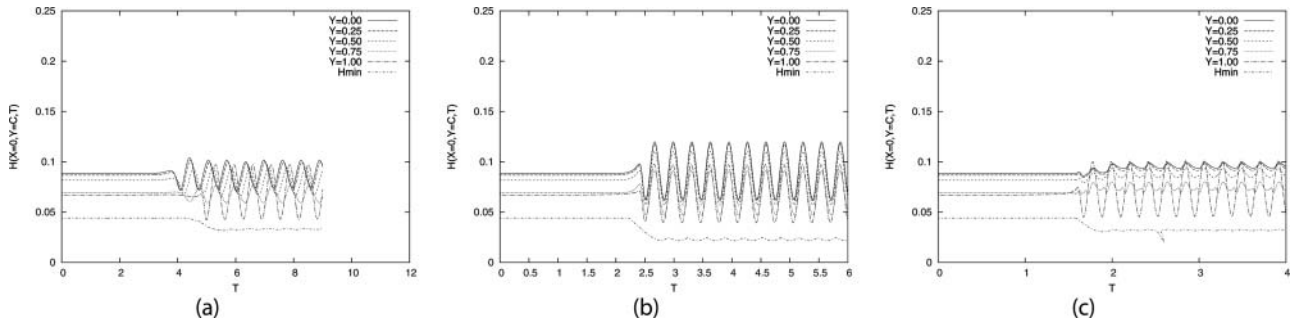

Fig. 20—Transverse waviness. Film thickness in the center of a point contact as a function of time at various spots transverse to the running direction, y = 0 is exactly in the middle, y = 1 is in the side lobes. From left to right: (a) rough surface is moving slower, (b) at equal speed, and (c) faster than the smooth surface (from Venner and Lubrecht *(177)*).

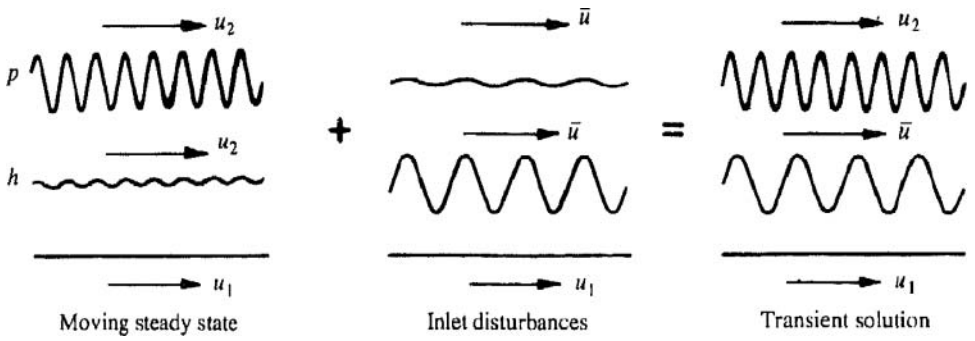

Fig. 21—Kinematics for a sinusoidal waviness in a EHL contact as proposed by the Morales–Espejl *(155), (104)* for rolling - sliding conditions and with Newtonian fluid.

only *(42)*, thus exploiting the similarities in the transverse and longitudinal amplitude reductions curves of Venner and Lubrecht *(40)*. The method applies a Fourier decomposition of the 3D topography, resolves for local film thickness and pressure fluctuations of each component, and then assembles back the results. A recent summary of the methodology with application to rolling bearings is given in Gabelli, et al. *(89)*.

Hooke *(128)*, by applying perturbation methods, has developed a fully analytical solution for sinusoidal waviness (extended to real roughness) that does not require the numerical results from Venner and Lubrecht. This analytical solution predicts very similar amplitude reduction curves as those numerically obtained.

Non-Newtonian Fluid

When the rheology of a non-Newtonian fluid is considered in the presence of sliding, several aspects of the physics change. The fluid viscosity needs to account for shear thinning effects. The contribution of the particular integral in the local film is not negligible anymore because considerable amplitude will remain. Thus, the amplitude reduction curves cannot directly be used to account for the missing amplitude in the complementary function. The complementary function will decay in amplitude as it enters into the contact and will propagate at the average speed of the surfaces.

Hooke, et al. *(128)*, *(129)* have developed a rapid method for the calculation of clearance and pressure fluctuations for 3D topography based on similar ideas as described for Newtonian fluids, taking into account the non-Newtonian behavior of the lubricant.

The model starts by considering the Reynolds equation,

$$\frac{\partial}{\partial x}\left(\frac{\rho h^3}{12\eta_x}\frac{\partial p}{\partial x}\right)+\frac{\partial}{\partial y}\left(\frac{\rho h^3}{12\eta_y}\frac{\partial p}{\partial y}\right)=\bar{u}\frac{\partial(\rho h)}{\partial x}+\frac{\partial(\rho h)}{\partial t} \qquad [60]$$

for an analysis at the center of the EHL contact, considering a sinusoidal waviness of amplitude r_a moving along x with speed u_2,

$$\delta r = r_a \exp(i\omega_x x)\exp(-i\omega_x u_2 t)\exp(i\omega_y y) \qquad [61]$$

where $\omega_x = 2\pi/\lambda_x$ and $\omega_y = 2\pi/\lambda_y$.

As the surfaces move, hydrodynamic pressures will be generated. Provided that the amplitude of the roughness is low, such pressures will be sinusoidal and will have the same wavelength—albeit not necessarily the same phase—as the undeformed roughness. Thus, they can be expressed as,

$$\delta p = p_a \exp(i\omega_x x)\exp(-i\omega_x u_2 t)\exp(i\omega_y y) \qquad [62]$$

where the imaginary part of the complex representation of the fluctuations δp is due to the differences in magnitude and phase between the original surface and the pressure fluctuation. These pressures will deform the elastic surface, creating elastic displacements on both surfaces that can be added. The surface deformation is superimposed on the original roughness to produce the clearance variation inside the contact,

$$\delta h = h_a \exp(i\omega_x x)\exp(-i\omega_x u_2 t)\exp(i\omega_y y) \qquad [63]$$

The pressure ripple will also change the density of the lubricant, and the change may be written as,

$$\delta\rho = \rho_a \exp(i\omega_x x)\exp(-i\omega_x u_2 t)\exp(i\omega_y y) \qquad [64]$$

where ρ_a is related to the pressure variation by

$$\rho_a = (\rho/B)p_a \qquad [65]$$

with B being the bulk modulus of the lubricant at a given pressure, $d\rho/dp = \rho/B$.

Now, because the amplitude of the variations is small, let us assume that products of fluctuations can be neglected in the Reynolds Eq. [60] as well as products of derivatives; therefore, the Reynolds equation can be written as

$$\frac{h^3}{12}\left(\frac{1}{\eta_x}\frac{\partial^2 p}{\partial x^2}+\frac{1}{\eta_y}\frac{\partial^2 p}{\partial y^2}\right)=\bar{u}\frac{\partial h}{\partial x}+\frac{\partial h}{\partial t}+\frac{h}{B}\left(\bar{u}\frac{\partial p}{\partial x}+\frac{\partial p}{\partial t}\right) \qquad [66]$$

Particular Integral

Pressure, clearance, and density variations can be added to the smooth contact and substituted in Eq. [66]; the equation simplifies to

$$\frac{\rho h^3\omega_x^2}{12\eta_x}p_a+\frac{\rho h^3\omega_y^2}{12\eta_y}p_a=i(u_2-\bar{u})\omega_x\left(\rho h_a+\frac{\rho h}{B}p_a\right) \qquad [67]$$

Solving for p_a, Eq. [67] leads to

$$\frac{p_a}{r_a}=\frac{\kappa E'}{4}\frac{iQ}{1-iQ-iCQ} \qquad [68]$$

where $\kappa = \sqrt{\omega_x^2 + \omega_y^2}$, $C = hE'\kappa/(4B)$ and

$$Q = \frac{\left(\frac{48(u_2-\bar{u})\omega_x}{E'h^3\kappa}\right)}{\left(\frac{\omega_x^2}{\eta_x} + \frac{\omega_y^2}{\eta_y}\right)}$$

For an Eyring fluid $\dot{\gamma} = \frac{\tau_0}{\eta}\sinh(\frac{\tau}{\tau_0})$ the effective viscosities *(83)* are

$$\eta_x = \frac{\eta}{\cosh(\tau_m/\tau_0)}$$
$$\eta_y = \frac{\eta(\tau_m/\tau_0)}{\sinh(\tau_m/\tau_0)} \qquad [69]$$

with τ_m being the mean shear stress.

Complementary Function

In the general problem of rolling–sliding, the complementary waves (pressures and clearance fluctuations) will decay in amplitude as they propagate in the contact due to the non-Newtonian effects from sliding. Hooke, et al. *(129)* suggested an exponential decay with respect to the inlet ($x' = x + a$) location. In addition, the complementary wave, because it propagates with the average speed of the lubricant, effectively will have a wavenumber in x such that $\omega_x' \approx \omega_x(u_2/\bar{u})$. Assuming that the wave decays exponentially with distance at a rate β, the amplitude of the clearance and by consequence the pressure can be expressed as:

$$\delta h_c = h_c \exp(i\psi x') \exp(-i\omega_x u_2 t) \exp(i\omega_y y)$$
$$\delta p_c = p_c \exp(i\psi x') \exp(-i\omega_x u_2 t) \exp(i\omega_y y) \qquad [70]$$

with $\psi = \omega_x' + i\beta$.

As mentioned before, the amplitude of the complementary function cannot be obtained only from the nominally parallel clearance assumption; here the inlet of the contact needs to be solved. Hooke, et al. *(129)* proposed a curve-fit solution from numerically obtained perturbation solutions for every wave component of the roughness.

Reference *(129)* gives some examples of rolling–sliding solutions for deterministic real surfaces, some of which have been used in actual experiments. For a single spherical asperity, the solution for pressure and deformed shape for different sliding–rolling rations as given in *(129)* are given in Fig. 22, where v is the sliding velocity and u is the entrainment speed of the lubricant in the contact. Measurements for film build–up and friction with various engineered surfaces can be found in Lugt et al. *(192)*.

Dimpled Surfaces

The impact of dimpled surfaces on tribological performance in fully flooded lubrication conditions has been studied in numerous papers. Akamatsu, et al. *(3)*, *(4)* were the first to publish a paper describing dimpled surface patterns that improve the life and degree of metallic contact under poor lubrication conditions, that is, low values of λ. Peeling tests carried out have shown that peeling appeared on superfinished specimens but not on specimens with isotropic patterns. The response to this work was given by Zhai, et al. *(188)*. They specifically investigated the surfaces from Akamatsu, et al. *(3)*, *(4)* and showed by calculations that the dimpled surfaces cannot improve film buildup in pure rolling. The film thickness would actually decrease adversely, affecting contact fatigue. They also mentioned that these dimpled surfaces would induce pressure spikes producing concentrated stresses around the dents, which would lead to surface cracks.

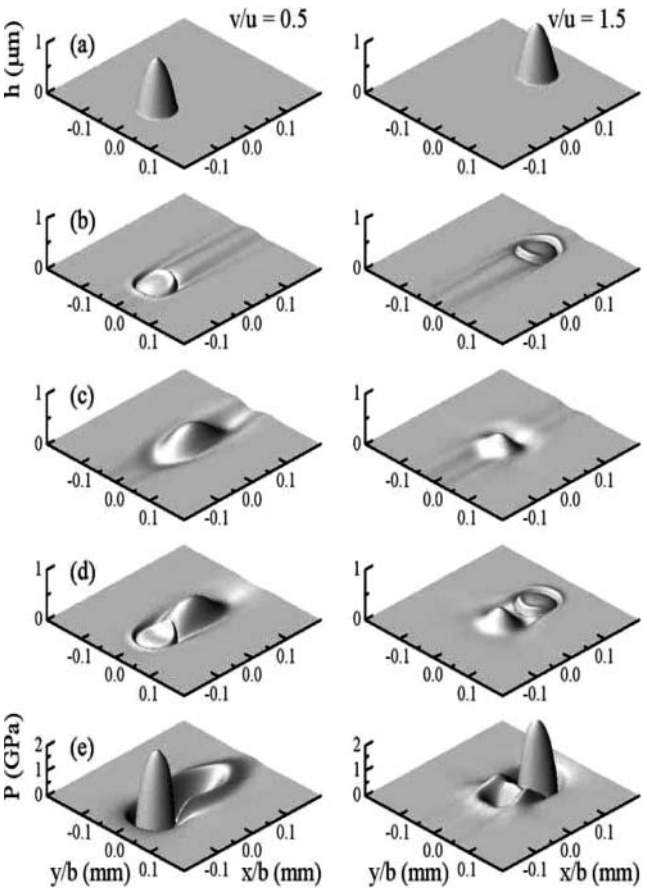

Fig. 22—Solution for 1 μm spherical asperity as reported by Hooke, et al. *(129)*: (a) undeformed profile, (b) attenuated roughness, (c) complementary wave, (d) combined clearance variation, and (e) pressure ripple, where *v* the is sliding velocity and *u* is the entrainment speed of the lubricant in the contact.

In 2000, Dumont, et al. *(80)* showed through numerical calculations that a positive effect of dimpled surfaces arises in the case of starved lubrication conditions. They calculated the film thickness in the contact by assuming a dimple geometry according to Fig. 23. In this configuration, the single pit present on one of the surfaces has a depth of 0.45 c, where c is the Hertzian mutal approach (1 μm). The pit is assumed to be filled with lubricant, so that outside the contact, the surface of the lubricant reaches a constant height equal to H_{oil} (see Fig. 23) above the nominal level of the pitted surface to which it adheres.

Figures 24 and 25 show the profile of the gap along the X axis on the centerline $Y = 0$ when the pit is located in the center of the contact. Comparison of the profiles obtained for fully flooded versus starved conditions shows that the reduction of amplitude of the pit itself is similar for both cases. To the contrary, a clear difference appears in the film profile behind and on the sides of the pit. For fully flooded conditions, Fig. 24 shows that the film profile around the pit is similar to the smooth film profile. For the starved conditions, changes in the film profile are visible

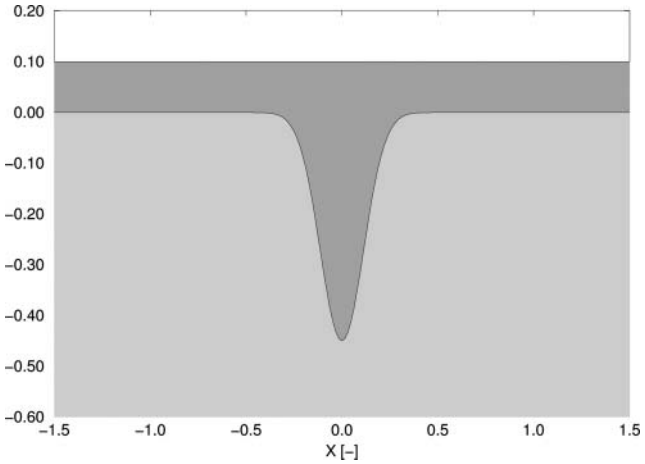

Fig. 23—Lubricant layer configuration for a dimple filled with oil.

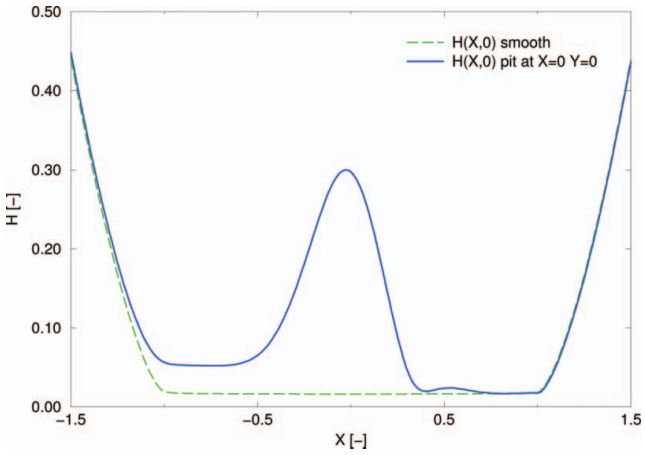

Fig. 25—Film thickness for a starved contact - Pit position at $X = 0$ $Y = 0$ - $H_{oil} = 0.02$

behind the pit (Fig. 25). Comparison of Figs. 24 and 25 shows that the film height behind the pit obtained under starved conditions tends for this case to the film height obtained for the fully flooded conditions. In the starved case the height of the film behind the pit is almost three times higher than the height in front of the pit, which does not differ much from the smooth starved film thickness. In the fully flooded case, Fig. 24 shows that the film behind the pit is hardly changed compared to the smooth fully flooded film thickness.

The calculations for fully flooded conditions from Zhai, et al. *(188)* and Dumont, et al. *(80)* were confirmed by Krupka, et al. *(146)* in 2008, who showed through film thickness measurements that dimpled surfaces are in general not beneficial to film buildup except for in the case of a large slip ratio (and where the dimples are on the faster moving surface) and at startup, which was earlier shown through calculations by Zhao and Sadeghi *(189)*.

FUTURE DEVELOPMENTS

From the recent literature, it is clear that modeling of tribological components has reached a high level of complexity. In the last decades single phenomena were studied, such as EHL and micro-EHL, fatigue, wear, surface heating, etc. In recent years the trend in modeling has been on integration of various aspects in tribology (e.g., micro-EHL as an input for surface fatigue and wear). Today, the challenge is no longer to predict single phenomena like film thickness or pressures but to study the interaction of several phenomena and, more important, their competitive nature. Moreover, there is a clear emphasis in modeling component failures *(84)*. In relation to EHL, detailed modeling of surface roughness interaction and its effects on fatigue in micro-EHL have recently been published, for example, Qiao, et al. *(164)*, *(165)* where the complete modeling of surface roughness movement in time is considered, including the mixed lubrication interactions and thermal effects. In another publication by the same group (Sharif, et al. *(170)*), a model for the wear phenomenon in gears under similar considerations was described. Lainé and Olver *(148)* modeled the competitive nature of two failure modes (micropitting and wear) on the surface of rolling–sliding EHL contacts, including the effect of lubricant additives; however, the pressures are still modeled using dry contact assumptions. Recent work, however, seems to show the possibility of numerically modelling micropitting considering mixed-lubrication pressures (Brandão, et al. *(27)*, *(29)*).

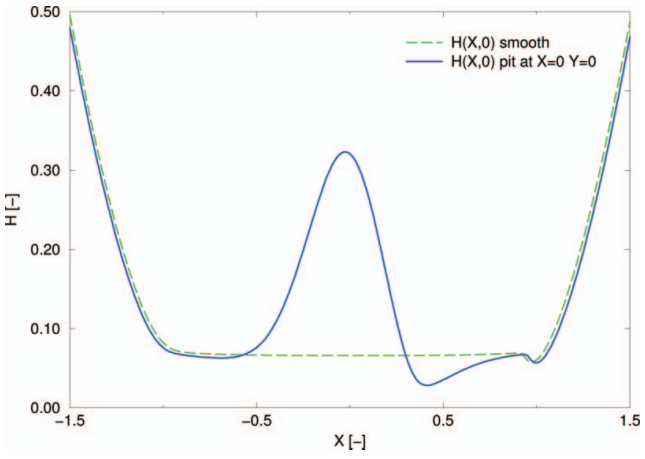

Fig. 24—Film thickness for a fully flooded contact - Pit position at $X = 0$ $Y = 0$.

An interesting development is CFD and the replacement of the Reynolds equation in EHL by the more complete physics of the Navier-Stokes equations (Almqvist *(5)*; Sahlin *(169)*; Hartinger, et al. *(120)*, *(52)*). This, in principle, would allow the direct modeling of cavitation, replenishment–starvation, turbulence, wall-slip, etc.

The modeling of roughness effects is also foreseen with this approach. However, it remains to be seen whether the computer time is eventually lowered to reasonable levels. Perhaps once again a logical solution would be to use these sophisticated methods to derive better semi-analytical formulae.

Work on starved EHL is progressing well. Today the film thickness and pressure in EHL can be predicted with great accuracy (Damiens *(34)*; Van Zoelen *(36)*). So far little work has been done on non-smooth surfaces in starved EHL. Especially in the case of starvation there is a risk of

film collapse, making this aspect important. Some work has been done by Venner, et al. *(176, 178)*, following the work from Chevalier *(32, 49)*. The same applies to non-Newtonian rheology and starved EHL. Yang, et al. *(186)* published work on line contacts. Work on, for example, elliptical contacts is still missing.

The main problem in starved EHL is the input on the inlet oil layer thickness. This is generally not known and research on this must therefore be connected to a specific application. An example is the application of starved EHL to rolling bearings by Van Zoelen et al. *(175)*. In addition, more research is needed on lubricant migration in the nonpressurized area. Here aspects of wetting, such as the Marangoni effect (Kien, et al. *(142)*), will need more attention.

For grease EHL, non-Newtonian models could be implemented in the existing EHL codes. However, grease consists of multiple components *(150)* for which indications exist that separation or layer formation in the contact will take place (Cann *(35)*). Moreover, grease rheology has a solid component, which makes it difficult to apply the existing EHL theory directly. This also applies to CFD techniques that are also based on fluid rheology. The two-component film will require a new approach.

Also, friction models for grease-lubricated contacts need to be developed. An important aspect is the (mechanical) aging of grease. The rheology of grease in EHL contacts cannot be taken as constant. An interesting start on modeling this phenomenon has been done by Merieux, et al. *(151)*. However, clearly much more work in this area is needed. This is also related to the development of good methods to measure grease rheology. The commonly used plate–plate or cone–plate measurement techniques may not be the best for measuring the highly nonlinear rheological behavior. Wall slip, cracking, leakage (Yeong, et al. *(187)*) and the assumption of a linear velocity profile between the instrument surfaces and many more phenomena make interpretation of rheological measurements very complex. Clearly there is still much work to be done here.

Another interesting area of development is molecular dynamics modeling. Especially important is the understanding of complex phenomena where traditional continuous mechanics approach cannot be used, either because the distance scales are extremely small (e.g., very thin films) or because of composite media with mixed properties (e.g., lubricant-air). Molecular dynamics has been used to model the chemical effects of boundary layers *(138)*, *(166)*.

Perhaps in the near future, the combined use of molecular dynamics simulations, thin-film fluid theory, and CFD will shine some light on the understanding of the real rheology of lubricants under EHL conditions (separating out thermal effects) and whether or not there is real wall-slip or failure of the lubricant by shear at the asperity summits as well as aid in the understanding of what the mechanisms are behind grease and boundary lubrication (interaction of lubricant and steel). It is possible that molecular dynamics modeling integrated into EHL can help engineers to understand one of the most important remaining problems in EHL: how the lubricating film actually fails.

ACKNOWLEDGEMENT

The authors thank A.J.C. de Vries, Director SKF Group Product Development, for his permission to publish this article.

REFERENCES

(1) Dowson, D. (1999), *History of Tribology*, John Wiley & Sons: New York.
(2) Reynolds, O. (1886), "On the Theory of Lubrication and Its Application to Mr. Beauchamp Tower's Experiments, Including Experimetal Determination of the Viscosity of Olive Oil," *Philosophical Transaction of the Royal Society*, **177**, pp 157-234.
(3) Akamatsu, Y., Tsushima, N., Goto, T., and Hibi, K. (1990), Improvement in Oil Film Formation Under Rolling Contact by Controlling Surface Roughness Pattern. *Proceedings of the Japan International Tribology Conference*, **2**, pp 761-766.
(4) Akamatsu, Y., Tsushima, N., Goto, T., and Hibi, K. (1992), "Influence of Surface Roughness Skewness on Rolling Contact Fatigue Life," *Tribology Transactions*, **35**(4), pp 571-582.
(5) Almqvist, T. (2004), *Computational Fluid Dynamics in Theoretical Simulations of Elastohydrodynamic Lubrication*, *Ph.D, Dissertation, Technical University of Lulea, Sweden*.
(6) Martin, H. M. (1916), "Lubrication of Gear Teeth," *Engineering*, **102**, pp 119-121.
(7) Gümbel, L. (1916), "Über Geschmierte Arbeitsräder" (On the Lubrication of Gears) *Zeitschrift fur das Gesamte Turbinenwesen*, **13**, p 357.
(8) Åström, H., Isaksson, O., and Höglund E. (1991), "Video Recordings of an EHL Point Contact Lubricated with Grease," *Tribology International*, **24**(3), pp 179-184.
(9) Meldahl, A. (1941), "Contribution to Theory of Lubrication of Gears and of Stressing of Lubricated Flanks of Gear Teeth," *Brown Boveri Review*, **28**(11), pp 374-382.
(10) von Mohrenstein-Ertel, A. (1949), "Die Berechnung der Hydrodynamischen Schmierung Gekrümmter Oberflächen unter Hoher Belastung und Relativbewegung," In *Fortschrittsberichte VDI*, Ser. 1, No. 115, Lang, O. R., and Oster, P. (Eds.), VDI Verlag: Düsseldorf. First Published in 1945 in Russian under the name A. M. Ertel.
(11) Åström, H., Östensen, J.-O., and Höglund, E. (1993), "Lubricating Grease Replenishment in an Elastohydrodynamic Point Contact," *Journal of Tribology*, **115**(3), pp 501-506.
(12) Grubin, A. N. (1949), "Investigation of the Contact of Machine Components," In Central Scientific Research Institute for Technology and Mechanical Engineering: Moscow, DSIR translation No. 337.
(13) Baart, P., Lugt, P. M., and Prakash, B. (2010), "Non-Newtonian Effects on Film Formation in Grease-Lubricated Radial Lip Seals," *Tribology Transactions*, **53**(3), pp 308-318.
(14) Cameron, A. (1985), "Righting a 40-Year-Old Wrong; A.M. Ertel–The True Author of Grubin's EHL Solution," *Tribology International*, **18**(2), p 92.
(15) Petrusevich, A. I. (1951), "Fundamental Conclusions from the Contact Hydrodynamic Theory of Lubrication," *Izvestiya Akademii Nauk SSSR (OTN)*, **3**(2), pp 209-223.
(16) Bair, S. (2007), *High-Pressure Rheology for Quantitative Elastohydrodynamics*. In *Tribology and Interface Engineering Series, 54*, Elsevier: The Netherlands.
(17) Baly, H., Poll, G., Cann, P. M., and Lubrecht, A. A. (2006), "Correlation between Model Test Devices and Full Bearing Tests under Grease Lubricated Conditions," *IUTAM Symposium on Elastohydrodynamics and Microelastohydrodynamics*, **134**(6), pp 229-240.
(18) Dowson, D., and Higginson, G. R. (1959), "A Numerical Solution to the Elasto-Hydrodynamic Problem," *Journal of Mechanical Engineering Science*, **1**, p 6.
(19) Dowson, D., and Higginson, G. R. (1966), *Elastohydrodynamic Lubrication: The Fundamentals of Roller and Gear Lubrication*, Pergamon: Oxford.
(20) Kauzlarich, J. J., and Greenwood, J. A. (1972), "Elastohydrodynamic Lubrication with Herschel-Bulkley Model Greases," *ASLE Transactions*, **15**(4), pp 269-277.
(21) Bauer, W. H., Finkelstein A. P., and Wiberley, S. E. (1960), "Flow Properties of Lithium Staerate-Oil Model Greases as a Function of Soap Concentration and Temperature," *ASLE Transactions*, **3**, pp 215-224.
(22) Hamrock, B. J., and Dowson, D. (1976), "Isothermal Elastohdrodynamic Lubrication of Point Contacts, Part I, Theoretical Formulation," *Journal of Tribology*, **98**, pp 223-229.

(23) Berthe, D., and Vergne, P. (1990), "High Pressure Rheology for High Pressure Lubrication: A Review," In *Journal of Rheology*, **34**, pp 1387-1414.

(24) Lubrecht, A. A., ten Napel, W. E., and Bosma, R. (1987), "Multigrid, an Alternative Method of Solution for Two-Dimensional Elastohydrodynamically Lubricated Point Contact Calculations," *Journal of Tribology*, **109**, pp 437-443.

(25) Bordenet, L., Dalmaz, G., Chaomleffel, J.-P., and Vergne, F. (1990), "A Study of Grease Film Thickness in Elastorheodynamic Rolling Point Contacts," *Lubrication Science*, **2**, pp 273-284.

(26) Yang, Z., and Qian, X. (1987), "A Study of Grease Film Thickness in Elastorheodynamic Rolling Point Contacts," *ImechE Conference Publication*, **1**(5), pp 97-104.

(27) Brand ao, J. A., Saebra, J. H. O., and Castro, J. (2010), "Surface Initiated Tooth Flank Damage Part I: Numerical Model," *Wear*, **268**, pp 1-12.

(28) Venner, C. H. (1991), *Multilevel Solution of the EHL Line and Point Contact Problems*, Ph.D. Thesis, University of Twente, Enschede, The Netherlands.

(29) Brand ao, J. A., Saebra, J. H. O., and Castro, J. (2010), "Surface Initiated Tooth Flank Damage. Part II: Prediction of Micropitting Initiation and Mass Loss," *Wear*, **268**, pp 13-22.

(30) Venner, C. H., and Lubrecht, A. A. (2000), *Multilevel Methods in Lubrication*, Elsevier: The Netherlands.

(31) Nijenbanning, G., Venner, C. H., and Moes, H. (1994), "Film Thickness in Elastohydrodynamically Lubricated Elliptic Contacts," *Wear*, **49**, pp 217-229.

(32) Chevalier, F., Lubrecht, A. A., Cann, P. M. E., Colin, F., and Dalmaz, G. (1998), "Film Thickness in Starved EHL Point Contacts," *Journal of Tribology*, **120**, pp 126-133.

(33) Cann, P. M. (1996), "Starvation and Reflow in a Grease-Lubricated Elastohydrodynamic Contact," *Tribology Transactions*, **39**(3), pp 698-704.

(34) Damiens, B., Venner, C. H., Cann, P. M., and Lubrecht, A. A. (2004), "Starved Lubrication of Elliptical EHD Contacts," *Journal of Tribology*, **126**(1), pp 105-111.

(35) Cann, P. M. (1999), "Starved Grease Lubrication of Rolling Contacts," *Tribology Transactions*, **42**(4), pp 867-873.

(36) van Zoelen, M. T., Venner, C. H., and Lugt, P. M. (2009), "Prediction of Film Thickness Decay in Starved Elasto Hydrodynamically Lubricated Contacts Using a Thin-Film Layer Model," *Proceedings of the Institution of Mechanical Engineers. Part J: Journal of Engineering Tribology*, **223**(3), pp 541-552.

(37) Cann, P. M., Hutchinson, J., and Spikes, H. A. (1996), "The Development of a Spacer Layer Imaging Method (Slim) for Mapping Elastohydrodynamic Contacts," *STLE Tribology Transactions*, **39**, pp 915-921.

(38) Zhu, D., and Hu, Y. (2001), "Effects of Rough Surface Topography and Orientation on the Characteristics of EHD and Mixed Lubrication in Both Circular and Elliptical Contacts," *Tribology Transactions*, **4**(3), pp 391-398.

(39) Cann, P. M., and Spikes, H. (1992), "Film Thickness Measurements of Lubricating Greases under Normally Starved Conditions," *NLGI Spokesman*, **56**(2), pp 21-27.

(40) Venner, C. H., and Lubrecht, A. A. (1999), "Amplitude Reduction of Non-Isotropic Harmonic Patterns in Circular EHL Contacts, under Pure Rolling," In *Lubrication at the Frontier, Proceedings of the 25th Leeds-Lyon Symposium on Tribology*, Elsevier Tribology Series 36 Dowson, D., et al. (eds.), Elsevier: The Netherlands, vol. 34, pp 151-162.

(41) Cheng, H. S. (1965), "A Refined Solution to the Thermal-Elastohydrodynamic Lubrication of Rolling and Sliding Cylinders," *ASLE Transactions*, **8**, pp 397-410.

(42) Morales-Espejel, G. E., Lugt, P. M., van Kuilenburg, J., and Tripp, J. H. (2003), "Effects of Surface Micro-Geometry on the Pressures and Internal Stresses of Pure Rolling EHL Contacts," *Tribology Transactions*, **46**, pp 260-272.

(43) Cheng, H. S. (1972), "Isothermal Elastohydrodynamic Theory in Full Range of Pressure/Viscosity Coefficient," *Transactions of the ASME Journal Lubrication Technology*, **94**, pp 35-43.

(44) Masen, M. A., Venner, C. H., Lugt, P. M., and Tripp, J. H. (2002), "Effects of Surface Micro-Geometry on the Lift-Off Speed of an EHL Contact," *Tribology Transactions*, **45**(1), pp 21-30.

(45) Cheng, H. S., and Sternlicht, B. (1965), "A Numerical Solution for the Pressure, Temperature and Film Thickness between two Infinitely Long, Lubricated Rolling and Sliding Cylinders, under Heavy Loads," *Journal of Basic Engineering*, **87**, pp 695-707.

(46) Spikes, H. A. (2006), "Sixty Years of EHL," *Lubrication Science*, **18**, pp 265-291.

(47) Dowson, D., and Ehret, P. (1999), "Past, Present and Future Studies in Elastohydrodynamics," *Proceedings of the Institution of the Mechanical Engineers, Part J*, **213**, pp 317-333.

(48) Chevalier, F. (1996), *Modélisation des conditions d'alimentation dans les contactes élastohydrodynamiques ponctuels*, Ph.D. Thesis, I. N.S.A. de Lyon, France.

(49) Chevalier, F., Lubrecht, A. A., Cann, P. M. E., Colin, F., and Dalmaz, G. (1995), "Starvation Phenomena in EHL Point Contacts: Influence of Inlet Flow Distribution," In *Lubricants and Lubrication, Procedings of the 21st Leeds-Lyon Symposium on Tribology, Elsevier Tribology Series 30*, Dowson, D., et al., (Eds.), Elsevier: The Netherlands, vol. 30, p 249257.

(50) van Odyck, D. E. A., and Venner, C. H. (2003), "Compressible Stokes Flow in Thin Films," *ASME Journal of Tribology*, **125**, p 543.

(51) Almqvist, T., and Larsson, R. (2002), "The Navier–Stokes Approach for Thermal EHL Line Contact Solutions," *Tribology International*, **35**(3), pp 163-170.

(52) Hartinger, M., Dumont, M. L., Ioannides, S., Gosman, D., and Spikes, H. (2008), "CFD Modeling of a Thermal and Shear-Thinning Elastohydrodynamic Line Contact," *Journal of Tribology*, **130**, p 041503.

(53) Chiu, Y. P. (1974), "An Analysis and Prediction of Lubricant Film Starvation in Rolling Contact Systems," *ASLE Transactions*, **17**, pp 22-35.

(54) Hertz, H. (1881), "Über die Berührung Fester Elasticher Körper," *Journal für die Reine und Angewandte Mathematik*, **92**, pp 156-171.

(55) Johnson, K. L. (1985), *Contact Mechanics*, Cambridge University Press: Cambridge.

(56) Couronné, I., Vergne, P., Ponsonnet, L., Truong-Dinh, N., and Girodin, D. (2000), "Influence of Grease Composition on Its Structure and Its Rheological Behaviour," *Proceedings of the Leeds-Lyon Conference, Thinning Films and Tribological Interfaces, Dowson, D., et al. (Eds.)*, pp 425-432, Elsevier: The Netherlands.

(57) Eyring, H. (1936), "Viscosity, Plasticity and Diffusion as Examples of Absolute Reaction Rates," *Journal of Chemical Physics*, **4**, 283-291.

(58) Karis, T. E., and Nagaraj, H. S. (2000), "Evaporation and Flow Properties of Several Hydrocarbon Oils," *Tribology Transactions*, **43**(4), pp 758-766.

(59) Crook, A. W.,(1961), "The Lubrication of Rollers, Part III," *Philosophical Transactions Royal Society London, Series A*, **254**, pp 237-258.

(60) Bogie, K., and Harris, J. (1968), "The Rheology of Greases I," *Rheologica Acta*, **7**(3), pp 255-260.

(61) Czarny, R., and Moes, H.,(1981), "Some Aspects of Lubricating Grease Flow," *Proceedings of the 3rd International Congress Tribology Eurotrib 8*, **3**, pp 68-85.

(62) Damiens, B. (2003), *Modelisation de la Lubrification Sous-Alimentee dans les Contactes Elastohydrodynamiques Elliptiques*, Ph.D. Thesis, Institut National des Sciences Appliquees de Lyon, France.

(63) Sánchez-Rubio, M., Chinas-Castillo, F., Ruiz-Aquino, F., and Lara-Romero, J. (2006), "A New Focus on the Walther Equation for Lubricant Viscosity Determination," *Lubrication Science*, **18**(2), pp 95-107.

(64) Seeton, C. J. (2006), "Viscosity-Temperature Correlation for Liquids," *Tribology Letters*, **22**(1), pp 67-78.

(65) Barus, C. (1893), "Isothermals, Isopiestics and Isometrics Relative to Viscosity," *American Journal of Science*, **45**, pp 87-96.

(66) Dong, D., and Qiang, X. (1988), "A Theory of Elastohydrodynamic Grease-Lubricated Line Contact Based on a Refined Rheological Model," *Tribology International*, **21**, pp 261-267.

(67) Dormois, H., Fillot, N., Habchi, W., Dalmaz, G., Vergne, P., Morales-Espejel, G. E., and Ioannides, E. (2010), "A Numerical Study of Friction in Isothermal EHD Rolling-Sliding Sphere-Plane Contacts with Spinning," *Journal of Tribology*, **132**, pp 021501-1-10.

(68) Roelands, C. J. A. (1966), *Correlational Aspects of the Viscosity–Temperature–Pressure Relationship of Lubricating Oils*, Ph.D. Thesis, Technische Hogeschool Delft, The Netherlands.

(69) Bair, S. (2001), "The Variation of Viscosity with Temperature and Pressure for Various Real Lubricants," *Journal of Tribology*, **123**(2), pp 433-437.

(70) Dormois, H., Fillot, N., Vergne, P., Dalmaz, G., Querry, M., Ioannides, E., and Morales-Espejel, G. E. (2009), "First Traction Results of High Spinning Large-Size Circular EHD Contacts From a New Test Rig: Tribogyr," *Tribology Transactions*, **52**, pp 171-179.

(71) Yasutomi, S., Bair, S., and Winer, W. (1984), "An Application of a Free Volume Model to Lubricant Rheology," *ASME Journal of Tribology*, **106**(2), pp 291-303.

(72) Liu, Q. (2002), *Friction in Mixed and Elastohydrodynamic Lubricated Contacts Including Thermal Effects*, Ph.D. Thesis, University of Twente, The Netherlands.

(73) Pirro, D. M., and Wessol, A. A. (2001), *Lubrication Fundamentals*, Mechanical Engineering, 2nd ed., Marcel Dekker: New York.

(74) Hamrock, B. J., and Dowson, D. (1976), "Isothermal Elastohdrodynamic Lubrication of Point Contacts, Part II—Ellipticity Parameter Results," *Journal of Tribology*, **98**(3), pp 375-383.

(75) Hamrock, B. J., and Dowson, D. (1977), "Isothermal Elastohdrodynamic Lubrication of Point Contacts, Part III—Fully Flooded Results," *Journal of Tribology*, **99**(2), pp 264-276.

(76) Dowson, D., Taylor, C. M., and Hu, X. (1986), "Elastohydrodynamic Lubrication of Elliptical Contacts with Pure Spin," In *Fluid Film Lubrication—Osborne Reynolds Centenary, Proceedings of the 13th Leeds-Lyon Symposium on Tribology, Leeds, UK, September 1986*, Dowson, D., Taylor, C. M., Godet, M., and Berthe, D. (Eds.) Elsevier: The Netherlands, pp 451-463.

(77) Chittenden, R. J., Dowson, D., Dunn, J., and Taylor, C. M. (1985), "A Theroretical Analysis of Isothermal EHL Concentrated Contacts: Parts I and II," *Proceeding Royal Society of London*, *A*, **397**(12), pp 245-294.

(78) Dowson, D., Taylor, C. M., and Xu, H. (1993), "Elastohydrodynamic Lubrication of Elliptical Contacts with Pure Spin," *Proceedings of the Institution Mechanical Engineers: Part C*, **207**, pp 83-92.

(79) Dowson, D., and Xu, H. (1991), "Elastohydrodynamic Lubrication of Elliptical Contacts with Spin and Rolling," *Proceedings of the Institution Mechanical Engineers: Part C*, **205**, pp 165-174.

(80) Dumont, M.-L., Lugt, P. M., and Tripp, J. H. (2002), "Surface Feature Effects in Starved Circular EHL Contacts," *Journal of Tribology*, **124**(2), pp 358-366.

(81) Dwyer-Joyce, R. S., Reddyhoff, T., and Drinkwater, B. W. (2004), "Operating Limits for Acoustic Measurement of Rolling Bearing Oil Film Thickness," *Tribology Transactions*, **47**, pp 366-375.

(82) Ehret, P., Dowson, D., and Taylor, C. M. (1996), "Waviness Orientation in EHL Point Contact," *Proceedings of the 22nd Leeds-Lyon Symposium of Tribology, Series* **31**, pp 235-244.

(83) Ehret, P., Dowson, D., and Taylor, C. M. (1998), "On Lubricant Transport Conditions in Elastohydrodynamic Conjunctions," *Philosophical Transactions Royal Society London, Series A*, **454**, pp 763-787.

(84) Evans, H. P., and Snidle, R. W. (2009), "The Future of Engineering Tribology in Concentrated Contacts," *Proceedings of the Institution of Mechanical Engineers: Part C*, **223**, pp 2939-2948.

(85) Evans, H. P., and Snidle, R. W. (1981), "Inverse Solution of Reynolds Equation of Lubrication under Point Contact Elastohydrodynamic Conditions," *Journal of Tribology*, **103**(4), pp 539-546.

(86) Evans, H. P., and Snidle, R. W. (1982), "The Elastohydrodynamic Lubrication of Point Contacts at Heavy Loads," *Proceedings of the Royal Society*, **A**, 382, pp 183-199.

(87) Félix-Quinonez, A. (2003), An Experimental and Theoretical Study of Elastohydrodynamically Lubricated Contacts with Well Defined Surface Features, *Ph.D. Thesis, University of Leeds*.

(88) Franke, J. E., and Poll, G. (1999), "Service Life and Lubrication Conditions of Different Grease Types in High-Speed Rolling Bearings," *In Lubrication at the Frontier (Tribology Series), Dowson, D. (Ed.)*, **36**, Elsevier: The Netherlands, pp 601-610.

(89) Gabelli, A., Morales-Espejel, G. E., and Ioannides, E. (2008), "Particle Damage in Hertzian Contacts and Life Ratings of Rolling Bearings," *Tribology Transactions*, **51**, pp 428-445.

(90) Okamura, H. (1982), "A Contribution to the Numerical Analysis of Isothermal Elastohydrodynamic Lubrication," In *Tribology of Reciprocating Engines, Proceedings of the 9th Leeds-Lyon Symposium on Tribology*, Elsevier Tribology Series Dowson, D., Taylor, C. M., Godet, M., and Berthe, D. (Eds.), Elsevier: The Netherlands, pp 313-320.

(91) Gecim, B., and Winer, W. O. (1981), "A Film Thickness Analysis for Line Contacts under Pure Rolling Conditions with a Non-Newtonian Rheological Model," *ASME Transactions, Journal of Lubrication Technology*, **103**, pp 305-316.

(92) Gershuni, L., Larson, M. G., and Lugt, P. M. (2008), "Replenishment in Rolling Bearings, *Tribology Transactions*, **51**, pp 643-651.

(93) Venner, C. H. (1990), "Advanced Multilevel Solution of the EHL Line Contact Problem," *Journal of Tribology*, **112**(3), pp 426-432.

(94) Lubrecht, A. A., ten Napel, W. E., and Bosma, R. (1986), "Multigrid, an Alternative Method of Solution for Two-Dimensional Elastohydrodynamically Lubricated Point Contact Calculations," *Journal of Tribology*, **108**(3), pp 551-558.

(95) Lubrecht, A. A. (1987), *Numerical Solution of the EHL Line and Point Contact Problem Using Multigrid Techniques*, Ph.D. thesis, University of Twente, Enschede, The Netherlands.

(96) Gohar, R., and Cameron, A. (1963), "Optical Measurement of Oil Film Thickness under Elastohydrodynamic Lubrication," *Nature*, **200**, p 458.

(97) Venner, C. H., and Ten Napel, W. E. (1992), "Advanced Multilevel Solution of the EHL Circular Contact Problem, Part 1: Theoretical Formulation and Algorithm," *Wear*, **152**(2),pp 351-367.

(98) Gohar, R., and Cameron, A. (1967), "The Mapping of Elastohydrodynamic Contacts," *ASLE Transactions*, **10**, pp 215-225.

(99) Venner, C. H., and Ten Napel, W. E. (1992), "Advanced Multilevel Solution of the EHL Circular Contact Problem, Part 2: Smooth Surface Results," *Wear*, **152**(2), pp 369-381.

(100) Brandt, A., and Lubrecht A. A. (1990), "Multilevel Matrix Multiplication and Fast Solution of Integral Equations," *Journal of Computational Physics*, **90**(2), pp 348-370.

(101) Greenwood, J. A., and Johnson, K. L. (1992), "The Behaviour of Transverse Roughness in a Sliding Elastohydrodynamically Lubricated Contact," *Wear*, **153**, pp 107-117.

(102) Greenwood, J. A., and Kauzlarich, J. J. (1973), "Inlet Shear Heating in Elastohydrodynamic Lubrication," *Transactions of the ASME, Journal of Lubrication Technology*, **95**, pp 417-426.

(103) Evans, H. P., and Hughes, T. G. (2000), "Evaluation of Deflexion in Semi-Infinite Bodies by a Differential Method," *Proceedings of the Institution Mechanical Engineers: Part C*, **214**, pp 563-584.

(104) Greenwood, J. A., and Morales-Espejel, G. E. (1994), "The Behaviour of Transverse Roughness in EHL Contacts," *Proceedings of the Institution of Mechanical Engineers: Part J*, **29**, pp 121-132.

(105) Holmes, M. J. A., Evans, H. P., Hughes, T. G., and Snidle, R. W. (2003), "Transient Elastohydrodynamic Point Contact Analysis Using a New Coupled Differential Defection Method Part 1: Theory and Validation," *Proceedings of the Institution of Mechanical Engineers: Part J*, **217**, pp 289-303.

(106) Holmes, M. J. A., Evans, H. P., Hughes, T. G., and Snidle, R. W. (2003), "Transient Elastohydrodynamic Point Contact Analysis Using a New Coupled Differential Defection Method Part 2: Results," In *Proceedings of the Institution of Mechanical Engineers: Part J*, **217**, pp 305-321.

(107) Holmes, M. J. A., Evans, H. P., and Snidle, R. W. (2005), "Analysis of Mixed Lubrication Effects in Simulated Gear Tooth Contacts," *ASME J. Lub. Tech.* **127**, pp 61-69.

(108) Guangteng, G. and Spikes, H. A. (1996), "The Role of Surface Tension and Disjoining Pressure in Starved and Parched Lubrication," *Proceedings of the Institution of Mechanical Engineers. Part J: Journal of Engineering Tribology*, **210**, pp 113-134.

(109) Guo, F., Yang, P., and Qu, S. (2001), "On the Theory of Thermal Elastohydrodynamic Lubrication at High Slide-Roll Ratios–Circular Glass-Steel Contact Solution at Opposite Sliding," *Transactions of the ASME, Journal of Tribology*, **123**, pp 816-821.

(110) Gupta, P. K., Cheng, H. S., Zhu, D., Fornster, N., and Schrand, J. (1991), "Visco-Elastic Effects in Mil-l-7808 Type Lubricant, Part I: Analytical Formulation," *Tribology Transactions*, **34**, pp 608-617.

(111) Gustafsson, L., Höglund, E., and Marklund, O. (1994), "Measuring Lubricant Film Thickness with Image Analysis," *Proceedings of the Institution of Mechanical Engineers: Part J*, **208**, pp 199-205.

(112) Habchi, W., Demirci, I., Eyheramendy, D., Morales-Espejel, G. E., and Vergne, P. (2007), "A Finite Element Approach of Thin Film Lubrication in Circular EHD Contacts," *ASME Journal of Tribology*, **40**, pp 1466-1473.

(113) Habchi, W., Eyheramendy, D., Vergne, P., and Morales-Espejel, G. E. (2008), "A Full-System Approach of the Elastohydrodynamic Line/Point Contact Problem," **130**, pp 021501-1-10.

(114) Habchi, W., Eyheramendy, D., Bair, S., Vergne, P., and Morales-Espejel, G. E. (2008), "Thermal Elastohydrodynamic Lubrication of Point Contacts Using a Newtonian/Generalized Newtonian Lubrication," *Tribology Letters*, **30**, pp 41-52.

(115) Habchi, W., Vergne, P., Bair, S., Andersson, O., Eyheramendy, D., and Morales-Espejel, G. E. (2010), "Influence of Pressure and Temperature Dependence of Thermal Properties of a Lubricant on the Behaviour of Circular TEHD Contacts," *Tribology International*, **43**, pp 1842-1850.

(116) Hamrock, B. J., and Dowson, D. (1977), "Isothermal Elastohdrodynamic Lubrication of Point Contacts, Part IV, Starvation Results," *Journal of Tribology*, **99**, pp 15-23.

(117) Greenwood, J. A. (1972), "An Extension of the Grubin Theory of Elastohydrodynamic Lubrication," *Journal of Physics D: Applied Physics*, **5**, pp 2195-2211.

(118) Hamrock, B. J., and Dowson, D. (1978), "Elastohydrodynamic Lubrication of Elliptical Contacts for Materials of Low Elastic Modulus 1–Fully Flooded Conjunction," *Journal of Tribology*, **100**, pp 236-245.

(119) Greenwood, J. A., and Morales-Espejel, G. E. (1995), "Pressure Spikes in EHL, In *Lubricants and Lubrication, Proceedings of the 21st Leeds-Lyon Symposium on Tribology*, Elsevier Tribology Series 30 Dowson, D. et al. (Eds.), Elsevier: Amsterdam, The Netherlands, vol. 30, pp 555-564.

(120) Hartinger, M., Gosman, D., Spikes, H. A., and Ioannides, E. (2008), "Two and Three-Dimensional CFD Modelling of Elastohydrodynamic Lubrication," In *Tribological Contacts and Component Life, Proceedings of the 34th Leeds-Lyon Symposium on Tribology, Elsevier Tribology Series 47, Dowson, D., et al. (Eds.), Elsevier: Amsterdam*.

(121) Christensen, H. (1979), "A Simplified Model of EHL of Rollers. The Central and Exit Solutions," *ASLE Transactions*, **22**, p 323.

(122) Crouch, R. F., and Cameron, A. (1961), "Viscosity-Temperature Equations for Lubricants," *Journal of the Institute of Petroleum*, **47**, pp 307-313.

(123) Heemskerk, R. S., Vermeiren, K. N., and Dolfsma, H. (1982), "Measurement of Lubrication Condition in Rolling Element Bearings," *ASLE Transactions*, **24**(4), pp 519-527.

(124) G. E. Morales-Espejel, G. E., and Wemekamp, A. W. (2008), "Ertel-Grubin Methods in Elastohydrodynamic Lubrication–a Review," *Proceedings of the Institution of Mechanical Engineers, Part J*, **222**, pp 15-34.

(125) Wolveridge, P. E., Baglin, K. P., and Archard, J. F. (1970-1971), "The Starved Lubrication of Cylinders in Line Contacts," *Proceedings of the Institution of Mechanical Engineers*, **185**, p 1159.

(126) Morales-Espejel, G. E. (2008), "Central Film Thickness in Time-Varying Normal Approach of Rolling Elastohydrodynamically Lubricated Contacts," *Proceedings of the Institution of Mechanical Engineers, Part C*, volume **222**, pp 1271-1280.

(127) Félix Quinonez, A., and Morales-Espejel, G. E. (2010), "Film Thickness Fluctuations in Time-Varying Normal Loading of Rolling Elastohydrodynamically Lubricated Contacts," *Proceedings of the Institution of Mechanical Engineers, Part C*, pp. 2559-2567.

(128) Hooke, C. J. (1998), "Surface Roughness Modification in Elastohydrodynamic Line Contacts Operating in the Elastic Piezoviscous Regime," Proceedings of the Institution of Mechanical Engineers: Part J, **212**, pp 145-162.

(129) Hooke, C. J., Li, Y. K., and Morales-Espejel, G. E. (2007), "Rapid Calculation of the Pressures and Clearances in Rolling-Sliding Elastohydrodynamically Lubricated Contacts, Part 2: General Non-Sinusoidal Roughness," *Proceedings of the Institution of Mechanical Engineers: Part C*, **221**, pp 555-564.

(130) Houpert, L., and Leenders, P. (1985), "A Theoretical and Experimental Investigation into Rolling Bearing Friction," In *EUROTRIB, Proceedings of the 4th European Tribology Congress*, Elsevier: Amsterdam.

(131) Jacobson, B. O., and Hamrock, B. J. (1983), "Non-Newtonian Fluid Model Incorporated into Elastohydrodynamic Lubrication of Rectangular Contacts," *NASA TM 83318*.

(132) Jacod, B. (2002), Friction in Elasto-Hydrodynamic Lubrication, Ph.D. Thesis, University of Twente, The Netherlands.

(133) Jacod, B., Publier, F., Cann, P. M. E., and Lubrecht, A. A. (1998), "An Analysis of Track Replenishment Mechanisms in the Starved Regime," In *25th Leeds-Lyon Symposium on Tribology, Elsevier Tribology Series*, Dowson, D., Priest, M., Taylor, C. M., Ehret, P., Childs, T. H. C., Dalmaz, G., Berthier, Y., Flamond, L., Georges, J. M–, Lubrecht, A. A. (Eds.) Elsevier: The Netherlands, vol. 36, pp 483-492.

(134) Jacod, B., Venner, C. H., and Lugt, P. M. (2001), "A Generalized Traction Curve for EHL Contacts," *Transactions of the ASME, Journal of Tribology*, **123**, pp 248-253.

(135) Jacod, B., Venner, C. H., and Lugt, P. M. (2003), "Extension of the Friction Mastercurve to Limiting Shear Stress Models," *Transactions of the ASME, Journal of Tribology*, **125**, pp 739-746.

(136) Jeng, Y.-R. (1990), "Experimental Study of the Effects of Surface Roughness on Friction," *Tribology Transactions*, **33**(3), pp 402-410.

(137) Jonkisz, W., and Krzemiński-Freda, H. (1979), "Pressure Distribution and Shape of an Elastohydrodynamic Grease Film," *Wear*, **55**, pp 81-89.

(138) Kamei, D., Zhou, H., Suzuki, K., Konno, K., Takami, S., Kubo, M., and Miyamoto, A. (2003), "Computational Chemistry Study on the Dynamics of Lubricant Molecules under Shear Conditions," *Tribology International*, **36**, pp 297-303.

(139) Kaneta, M., Kanada, T., and Nishikawa, H. (1997), "Optical Interferometric Observations of the Effects of a Moving Dent on Point Contact EHL," In *Elastohydrodynamics 96, Proceedings of the 23rd Leeds-Lyon Symposium on Tribology, Elsevier Tribology Series 32, Dowson, D., Taylor, C. M., Childs, T. H. C., Dalmaz, G., Berthier, Y., Flamand, L., Georges, J.M–, Lubrecht, A. A. (Eds.)*, Elsevier: The Netherlands, vol. 32, pp 69-79.

(140) Kaneta, M., Ogata, T., Takubo, Y., and Naka, M. (2000), "Effects of Thickener Structure on Grease Elastohydrodynamic Lubricant Films," *Proceedings of the Institution of Mechanical Engineers: Part J., Journal of Engineering Tribology*, **214**, pp 327-336.

(141) Kaneta, M., Sakai, T., and Nishikawa, H. (1993), "Effects of Surface Roughness on Point Contact EHL," *Tribology Transactions*, **36**(4), pp 605-612.

(142) Kien, S., Surberg, C. H., Stehr, W., and Köttrich, H. (2008), "Influences of Lubricants and Surface Topographies on Marangoni Phenomena," In *Technische Akademi Esslingen International Tribology Colloquium Proceedings*, Bartz, W. J. (Ed.), vol. 16.

(143) Kim, H. J., Ehret, P., Dowson, D., and Taylor, C. M. (2001), "Thermal Elastohydrodynamic Analysis of Circular Contacts. Part 2: Non-Newtonian Model," *Proceedings of the Institution of Mechanical Engineers: Part J*, **215**, pp 353-362.

(144) Kim, K. M., and Sadeghi, F. (1992), "Three-Dimensional Temperature Distribution in EHD Lubrication: Part I–Circular Contact," In *Transactions of the ASME, Journal of Tribology*, **114**, pp 32-41.

(145) Kingsbury, E. (1985), "Parched Elastohydrodynamic Lubrication," *Journal of Tribology*, **107**, pp 229-233.

(146) Krupka, I., and Hartl, M. (2007), "The Effect of Surface Texturing on Thin EHD Lubrication Films," *Tribology International*, **40**, pp 1100-1110.

(147) Krupta, I., Hartl, M., Poliscuk, R., Cermak, J., and Liska, M. (2000), "Experimental Evaluation of EHD Film Shape and Its Comparison with Numerical Solution," *Transactions of the ASME, Journal of Tribology*, **122**, pp 689-696.

(148) Lainé, E., and Olver, A. V. (2007), "The Effect of Anti-Wear Additives on Fatigue Damage," *Extended Abstract, STLE 62nd Meeting*, Philadelphia, PA.

(149) Liu, X., Jiang, M., Yang, P., and Kaneta, M. (2005), "Non-Newtonian Thermal Analyses of Point EHL Contacts Using and Eyring Model," *Transactions of the ASME, Journal of Tribology*, **127**, pp 70-81.

(150) Lugt, P. M. (2009), "A Review on Grease Lubrication in Rolling Bearings," *Tribology Transactions*, **52**(4), pp 470-480.

(151) Mérieux, J.-S., Hurley, S., Lubrecht, A. A., and Cann, P. M. (2000), "Shear-Degradation of Grease and Base Oil Availability in Starved EHL Lubrication," In *Proceedings of the 26th Leeds-Lyon Symposium on Tribology*, Dowson, D., Taylor, C. M., Childs, T. H. C., Dalmaz, G., Berthier, Y., Flamand, L., Georges, J.M–, Lubrecht, A. A. (Eds.), Elsevier: Amsterdam, The Netherlands, Tribology Series, vol. 38, pp 581-588.

(152) Moes, H. (1965), "Discussion on a Paper by D. Dowson," *Proceedings of the Institution of Mechanical Engineers*, **180**, pp 294-295.

(153) Moes, H. (1992), "Optimum Similarity Analysis with Applications to Elastohydrodynamic Lubrication," *Wear*, **159**, pp 57-66.

(154) Molimard, J., Querry, M., and Vergne, P. (1998), "New Tools for the Experimental Study of EHD and Limit Lubrication," In *Thinning Films and Tribological Interface, Proceedings of the 26th Leeds-Lyon Symposium on Tribology*, Elsevier Tribology Series 36, Dowson, D., Priest, M., Taylor, C. M., Ehret, P., Childs, T. H. C., Dalmaz, G., Berthier, Y., Flamond, L., Georges, J. M–, Lubrecht, A. A. (Eds.) Elsevier: The Netherlands, vol. 37, pp 717-726.

(155) Morales-Espejel, G. E. (1993), *Elastohydrodynamic Lubrication of Smooth and Rough Surfaces*, Ph.D. Thesis, University of Cambridge, U.K.

(156) Morales-Espejel, G. E., and Wemekamp, A. W. (2004), "An Engineering Approach on Sliding Friction in Full-Film, Heavily Loaded Lubricated Contacts," *Proceedings of the Institution of Mechanical Engineers, Part J*, **218**, pp 513-528.

(157) Yang P. and Cui, J. (2004), "The Influence of Spinning on the Performance of EHL in Elliptical Contacts," In *IUTAM Symposium on Elastohydrodynamics and Micro-Elastohydrodynamics, Cardiff, U.K., September 2004*, pp 81-92.

(158) Patir, N., and Cheng, H. S. (1978), "An Average Flow Model or Determining Effects of Three-Dimensional Roughness on Partial Hydrodynamic Lubrication," *Journal of Tribology*, **100**, pp 12-17.

(159) Pemberton, J., and Cameron, A. (1976), "A mechanism of Fluid Replenishment in Elastohydrodynamic Contacts," *Wear*, **37**, pp 184-190.

(160) Poon, S. Y. (1970-1971), "Some Calculations to Assess the Effect of Spin on the Tractive Capacity of the Rolling Contact Drives," *Proceedings of the Institution of Mechanical Engineers*, **185**, pp 1015-1022.

(161) Poon, S. Y. (1972), "Experimental Study of Grease in Elastohydrodynamic Lubrication," *Journal of Lubrication Technology*, **94**(1), pp 27-34.

(162) Popovici, G. (2005), *Effects of Lubricant Starvation on Performance of Elasto-Hydrodynamically Lubricated Contacts*, Ph.D. Thesis, University of Twente, Enschede, The Netherlands.

(163) Zou Q., Huang, C., and Wen, S. (1999), "Elastohydrodynamic Film Thickness in Elliptical Contacts with Spinning and Rolling," *Transactions of the ASME, Journal of Tribology*, **121**, pp 686-692.

(164) Qiao, H. (2006), Prediction of Contact Fatigue for the Elastohydrodynamic Lubrication Line Contact Problem under Rolling & Sliding Conditions, Ph.D. Dissertation, University of Cardiff, UK.

(165) Qiao, H., Evans, H. P., and Snidle, R. W. (2008), "Comparison of Fatigue Model Results for Rough Surface Elastohydrodynamic Lubrication," Proceedings of the Institution of Mechanical Engineers, Part J, **222**, pp 381-393.

(166) Rajendran, A., Takahashi, Y., Koyama, M., Kubo, M., and Miyamoto, A., (2004), "Tight-Binding Quantum Chemical Molecular Dynamics Simulation of Mechano-Chemical Reactions During Chemical Mechanical Polishing Process of SiO_2 Surface by CeO_2 Particle," *Appllied Surface Science*, **244**, pp 34-38.

(167) Reddyhoff, T., Spikes, H. A., and Olver, A. V. (2009), "Improved Infrared Temperature Mapping of Elastohydrodynamic Contacts," *Proceedings of the Institution of Mechanical Engineers: Part J*, **223**, pp 1165-1177.

(168) Snidle, R. W., and Archard, J. F. (1969-1970), "Theory of Hydrodynamic Lubrication for a Spinning Sphere," *Proceedings of the Institution of Mechanical Engineers: Part 1*, **184**(44), pp 839-846.

(169) Sahlin, F. (2008), Lubrication, Contact Mechanics and Leakage Between Rough Surfaces, Ph.D. Dissertation, Technical University of Lulea, Sweden.

(170) Sharif, K. J., Evans, H. P., and Snidle, R. W. (2006), "Wear Modelling of Worm Gears," In *IUTAM Symposium on Elastohydrodynamics and Microelastohydrodynamics*, Snidle, R. W., Evans, H. P. (Eds.), Springer: UK, pp 371-383.

(171) Taniguchi, M., Dowson, D., and Taylor, C. M. (1996), "The Effect of Spin Motion upon Elastohydrodynamic Elliptical Contacts," In *Elastohydrodynamics 96, Proceedings of the 23rd Leeds-Lyon Symposium on Tribology*, Elsevier Tribology Series 32, Dowson, D., et al. (Eds.), Elsevier: Amsterdam, pp 599-610.

(172) Tevaarwerk, J. L., and Johnson, K. L. (1979), "The Influence of Fluid Rheology on the Performance of Traction Drives," *Transactions of the ASME Journal of Lubrication Technology*, **101**, pp 266-274.

(173) Van Zoelen, M. T. (2010), *Thin Layer Flow in Rolling Element Bearings*, Ph.D. Thesis, University of Twente, The Netherlands.

(174) van Zoelen, M. T., Venner, C. H., and Lugt, P. M. (2008), "Free Surface Thin Layer Flow on Bearing Raceways," *Journal of Tribology*, **130**(2), pp 021802-1-021802-10.

(175) van Zoelen, M. T., Venner, C. H., and Lugt, P. M. (2010), "The Prediction of Contact Pressure Induced Film Thickness Decay in Starved Lubricated Rolling Bearings," *Tribology Transactions*, **53**(6), pp 831-841.

(176) Venner, C. H., Berger, G., and Lugt, P. M. (2004), "Waviness Deformation in Starved EHL Circular Contacts," *Journal of Tribology*, **126**(2), pp 248-257.

(177) Venner, C. H., and Lubrecht, A. A. (1996), "Numerical Analysis of the Influence of Waviness on the Film Thickness of a Circular EHL Contact," *Journal of Tribology*, **118**, pp 153-161.

(178) Venner, C. H., Popovici, G., Lugt, P. M., and Organisciak, M. (2008), "Film Thickness Modulations in Starved Elastohydrodynamically Lubricated Contacts Induced by Time-Varying Lubricant Supply," *Journal of Tribology*, **130**(4), p 041501.

(179) Vergne, P. (2007), "Mapping in Situ Dynamic Thin Films by Optical Techniques," In *AFI/TFI-2007, Commemoration of the 100th Anniversary of Tohoku University December 14-15, 2007*, Sendai, Miyagi, Japan, pp 166-173.

(180) Vergne, P., and Ville, F. (2006), "Experimental Investigation on the Pressure Distribution for Pure Sliding EHL Contacts with Dented Surfaces," In *IUTAM Symposium on Elastohydrodynamics and Micro-Elastohydrodynamics, Snidle, R. W., and Evans, H. P. (Eds.)*, Springer: UK, pp 201-213.

(181) Wang, S., Cusano, C., and Conry, T. F. (1991), "Thermal Analysis of Elastohydro-Dynamic Lubrication of Line Contacts Using the Ree-Eyring Fluid Model," *Journal of Tribology*, **113**, pp 232-244.

(182) Wedeven, L. D., Evans, D., and Cameron, A. (1971), "Optical Analysis of Ball Bearing Starvation," *Journal of Tribology*, **93**, pp 349-363.

(183) Wijnant, Y. H. (2005), *Contact Dynamics in the Field of Elastohydrodynamic Lubrication*, Ph.D. Thesis, University of Twente, Enschede, The Netherlands.

(184) Williamson, B. P., Kendall, D. L. R., and Cann, P. M. (1993), "The Influence of Grease Composition on Film Thickness in EHD Contacts," *NLGI Spokesman*, **57**(8), pp 13-18.

(185) Wolveridge, P. E., Baglin, K. P., and Archard, J. F. (1971), "The Starved Lubrication of Cylinders in Line Contact," *Proceedings of the Institution of Mechanical Engineers*, **181**, pp 1159-1169.

(186) Yang, P., Wang, J., and Kaneta, M. (2006), "Thermal and Non-Newtonian Numerical Analyses for Starved EHL Line Contacts," *Journal of Tribology*, **128**, pp 282-290.

(187) Yeong, S. K., Luckham, P. F., and Tadros, Th. F. (2004), "Steady Flow and Viscoelastic Properties of Lubricating Grease Containing Various Thickener Concentrations," *Journal of Colloid and Interface Science*, **274**, pp 285-293.

(188) Zhai, X. Z., Chang, L., Hoeprich, M. R., and Nixon, H. P. (1997), "On Mechanisms of Fatigue Life Enhancement by Surface Dents in Heaviliy Loaded Rolling Line Contacts," *Tribology Transactions*, **40**(4), pp 708-714.

(189) Zhao, J., and Sadeghi, F. (2004), "The Effects of a Stationary Surface Pocket on EHL Line Contact Start-Up," *Journal of Tribology*, **126**(4), pp 672-680.

(190) Zhu, D., and Wen, S. (1984), "A Full Numerical Solution for the Thermal-Elastohydrodynamic Problem in Elliptical Contacts," *Transactions of the ASME, Journal of Tribology*, **106**, pp 246-254.

(191) Zhu, W. S., and Neng, Y. T. (1988), "A Theoretical and Experimental Study of EHL Lubricated with Grease," *Journal of Tribology*, **110**, pp 38-43.

(192) Lugt, P. M., Severt, R. W. M., Fogelstroem, J., and Tripp, J. H. (2001), "Influence of surface topography on friction, film break–down, and running–in the mixed lubrication regime", *Proceedings of the Institution of Mechanical Engineers. Part J: Journal of Engineering Tribology*, **215**, pp 519-533.